

Supporting Information for

Catalytic dehydrocoupling of amine-boranes and amines into diaminoboranes.

Isolation of a Pt(II), Shimoi-type, η^1 -BH complex.

Marta Roselló-Merino,^a Raquel J. Rama,^a Josefina Díez,^b Salvador Conejero^{a,*}

^[a] *Instituto de Investigaciones Químicas (IIQ), Departamento de Química Inorgánica, Centro de Innovación en Química Avanzada (ORFEO-CINQA), CSIC / Universidad de Sevilla, Avda. Américo Vespucio 49, 41092 Sevilla (Spain).*

^[b] *Departamento de Orgánica e Inorgánica, Centro de Innovación en Química Avanzada (ORFEO-CINQA), Universidad de Oviedo, C/ Julián Clavería 8, 33006, Oviedo (Spain)*

Contents:

1. General	S1
2. Synthesis and spectroscopic data for diaminoboranes	S3
3. NMR spectra of diaminoboranes	S9
4. NMR spectra of complex [Pt(I^tBu')(I^tBu)][BAR^F] (3c) at 298 and 183 K	S29
5. NMR spectra of a mixture of complex [PtH(I^tBu)₂][BAR^F] (4) and H₃B·C₅H₅N at 298 and 188 K	S32
6. H₂ Evolution graphics in a closed reaction vessel	S36
7. X-ray crystal structure determination of complex 3c	S40
8. References	S41

1. General. The NMR instruments were Bruker DRX-500, DRX-400 and DPX-300 spectrometers. Spectra were referenced to external SiMe₄ (δ 0 ppm) using the residual protio solvent peaks as internal standard (¹H NMR experiments) or the characteristic

resonances of the solvent nuclei (^{13}C NMR experiments). Spectral assignments were made by routine one- and two-dimensional NMR experiments where appropriate. Amine-boranes $\text{NMe}_2\text{H}\cdot\text{BH}_3$ and $\text{N}^i\text{BuH}_2\cdot\text{BH}_3$ were purchased from Aldrich, used as received. $\text{NEt}_2\text{H}\cdot\text{BH}_3$, $(\text{CH}_2)_4\text{NH}\cdot\text{BH}_3$ and $\text{C}_5\text{H}_5\text{N}\cdot\text{BH}_3$ were synthesized in CH_2Cl_2 from NEt_2H , $(\text{CH}_2)_4\text{NH}$ or pyridine and $\text{Me}_2\text{S}\cdot\text{BH}_3$, following a synthetic protocol similar to that described by as described by Neümuller.¹ All manipulations were performed under dry, oxygen-free argon, following conventional Schlenk techniques. Complexes $[\text{Pt}(i\text{Bu})(i\text{Bu})][\text{BAR}^F]$ (**1**),^[2] $[\text{PtH}(i\text{Bu})_2][\text{BAR}^F]$ ^[3] (**2**) and $[\text{Pt}(i\text{Bu})(i\text{Bu})(\text{H}_3\text{B}\cdot\text{NHMe}_2)][\text{BAR}^F]$ (**3a**)^[4] were obtained accordingly to published procedures.

H_2 evolution was measured using a Man on the Moon series X102 kit,^[5] which monitors the variation of pressure and temperature of the gas phase inside a closed reaction flask.¹ The reaction flask is connected to a switchable 3-way valve via a Thorion screw through polyamide tubing. The valve can be switched between two positions, one of them connecting the reactor vessel to the exterior so that it can be used like a conventional Schlenk flask. The other position connects the flask to the pressure transducer, thus closing the system. The assembled device is depicted in Figure S1.



Figure S1. Man on the moon series X102 kit1

¹ www.manonthemoontech.com

2. Synthesis and spectroscopic data for diaminoboranes

2.1 Catalytic reactions leading to symmetric (NRR')₂BH in a man-on-the-moon flask with catalyst 1.

In a typical procedure, the amine (NRR'H, 0.276 mmol) and its amine-borane counterpart (NRR'H·BH₃, 0.276 mmol) are dissolved in 0.5 mL of CH₂Cl₂ (or CD₂Cl₂) in a 35 mL flask. Thereafter, the pressure inside is allowed to stabilize and a solution of complex **1** (1.95 mg in 50 μL of CH₂Cl₂ or CD₂Cl₂, 0.00138 mmol) prepared immediately before use is injected and the pressure inside the flask measured at intervals of 1.38 s, until no increase in the internal pressure is observed. Conversions were determined by both the amount of H₂ released (using the ideal gas law $P \cdot V = n \cdot R \cdot T$, where V is the volume of the flask minus the volume of solvent used) and by ¹¹B and ¹H NMR spectroscopy (see below).

2.2 Catalytic reactions leading to symmetric (NRR')₂BH with catalyst 1 in a preparative scale.

In a typical procedure, the amine (NRR'H, 0.552 mmol) and its amine-borane counterpart (NRR'H·BH₃, 0.552 mmol) are dissolved in 0.9 mL of CH₂Cl₂. Thereafter, a solution of complex **1** (3.9 mg in 100 μL of CH₂Cl₂, 0.00276 mmol), prepared immediately before use, is injected. The reaction is stirred at room temperature until no gas evolution is observed (in some of the cases, at the very end of the reaction the initial colorless solution becomes pale yellow as a consequence of the presence of complex **1**). The volatile fraction of the reaction mixture is then transferred trap-to-trap into a Young tube at high-vacuum (*ca.* 5 × 10⁻³ bar), and the CH₂Cl₂ of this solution (that contains the diaminoborane) is evaporated to dryness at -30 °C, leading to a colorless oil. The diaminoboranes proved to be moisture sensitive (in some cases, a broad signal at *ca.* 20 ppm is observed in the ¹¹B NMR spectra due to trace amounts of hydrolysis products). All attempts to obtain satisfactory elemental analysis or mass spectra failed.

2.3 Catalytic reactions leading to asymmetric (NR^aR^b)(NR^cR^d)₂BH in a man-on-the-moon flask with catalyst 1.

In a typical procedure, amine-borane (NR^aR^bH·BH₃, 0.276 mmol) is dissolved in 0.4 mL of CH₂Cl₂ (or CD₂Cl₂) in a 35 mL flask. Thereafter, the pressure inside is allowed to stabilize and a solution of complex **1** (1.95 mg, 0.00138 mmol) and the amine (NR^cR^dH, 0.276 mmol) in 100 μL of CH₂Cl₂ (or CD₂Cl₂) prepared immediately before

use is injected and the pressure inside the flask measured at intervals of 1.38 s, until no increase in the internal pressure is observed. Conversions were determined by both the amount of H₂ released released (using the ideal gas law $P \cdot V = n \cdot R \cdot T$, where V is the volume of the flask minus the volume of solvent used) and by ¹¹B and ¹H NMR spectroscopy (see below).

2.4 Catalytic reactions leading to symmetric (NRR')₂BH with catalyst **1** in preparative scale.

In a typical procedure, and the amine-borane (NR^aR^bH·BH₃, 0.552 mmol) is dissolved in 0.9 mL of CH₂Cl₂. Thereafter, a solution of complex **1** (3.9 mg., 0.00276 mmol) and the amine (NR^cR^dH, 0.552 mmol) in 100 μL of CH₂Cl₂, prepared immediately before use, is injected. The reaction is stirred at room temperature until no gas evolution is observed (in some of the cases, at the very end of the reaction the initial colorless solution becomes pale yellow as a consequence of the presence of complex **1**). The reaction mixture is then transferred trap-to-trap into a Young tube at high-vacuum (*ca.* 5 x 10⁻³ bar), and the CH₂Cl₂ of this solution (that contains the diaminoborane) is evaporated to dryness at -30 °C, leading to a colorless oil.

Diaminoborane (N^tBuH)₂BH. The general procedure described in section 2.2 using N^tBuH₂·BH₃ and N^tBuH₂ was followed, leading to 85 mg (99% yield) of the diaminoborane.

NMR data in C₆D₆:

¹¹B NMR (128 MHz, C₆D₆, 298 K): δ 25.8 (d, ¹J_{B,H} = 126 Hz). ¹H{¹¹B} NMR (400 MHz, C₆D₆, 298 K): δ 4.39 (t, J_{H,H} = 8.2 Hz, 1H, BH), 2.43 (br, 2H, NH), 1.15 (s, 18H, CH₃). ¹³C{¹H} NMR (101 MHz, C₆D₆, 298 K): δ 48.5 (s, C(CH₃)₃), 33.3 (s, C(CH₃)₃).

NMR data in CD₂Cl₂:

¹¹B NMR (128 MHz, CD₂Cl₂, 298 K): δ 25.8 (d, ¹J_{B,H} = 126 Hz). ¹H{¹¹B} NMR (300 MHz, CD₂Cl₂, 298 K): δ 4.09 (t, J_{H,H} = 8.2 Hz, 1H, BH), 2.74 (br, 2H, NH), 1.14 (s, 18H, CH₃). ¹³C{¹H} (101 MHz, CD₂Cl₂, 298 K): δ 48.7 (s, C(CH₃)₃), 33.3 (s, C(CH₃)₃).

Diaminoborane (NEt₂)₂BH. The general procedure described in section 2.2 using NEt₂H·BH₃ and NEt₂H was followed, leading to 76 mg (88% yield) of the diaminoborane.

NMR data in C₆D₆:

^{11}B NMR (128 MHz, C_6D_6 , 298 K): δ 28.8 (d, $^1J_{\text{B,H}} = 125$ Hz). $^1\text{H}\{^{11}\text{B}\}$ NMR (400 MHz, C_6D_6 , 298 K): δ 4.07 (s, 1H, BH), 2.96 (q, 8H, $J_{\text{H,H}} = 7.0$ Hz, NCH_2CH_3), 1.01 (t, 12H, $J_{\text{H,H}} = 7.0$ Hz, NCH_2CH_3). $^{13}\text{C}\{^1\text{H}\}$ NMR (101 MHz, C_6D_6 , 298 K): δ 44.4 (s, NCH_2CH_3), 17.0 (s, NCH_2CH_3).

NMR data in CD_2Cl_2 :

^{11}B NMR (128 MHz, CD_2Cl_2 , 298 K): δ 28.5 (d, $^1J_{\text{B,H}} = 125$ Hz). $^1\text{H}\{^{11}\text{B}\}$ NMR (400 MHz, CD_2Cl_2 , 298 K): δ 3.70 (s, 1H, BH), 2.98 (q, 8H, $J_{\text{H,H}} = 7.0$ Hz, NCH_2CH_3), 1.04 (t, 12H, $J_{\text{H,H}} = 7.0$ Hz, NCH_2CH_3).

Diaminoborane $[\text{N}(\text{CH}_2)_4]_2\text{BH}$. The general procedure described in section 2.2 using $\text{N}(\text{CH}_2)_4\text{H}\cdot\text{BH}_3$ and $\text{N}(\text{CH}_2)_4\text{H}$ was followed but due to its higher boiling point, a different protocol was used to obtain it. At the end of the reaction, CH_2Cl_2 was removed under vacuum and diaminoborane $[\text{N}(\text{CH}_2)_4]_2\text{BH}$ was extracted with dry pentane (4 mL) leading to 68 mg (81% yield) of the diaminoborane after solvent evaporation contaminated with some hydrolysis species (see Figure S12).

NMR data in C_6D_6 :

^{11}B NMR (160 MHz, C_6D_6 , 298 K): δ 26.8 (d, $^1J_{\text{B,H}} = 127$ Hz). $^1\text{H}\{^{11}\text{B}\}$ NMR (400 MHz, C_6D_6 , 298 K): δ 4.42 (s, 1H, BH), 3.29 (m, 8H, NCH_2CH_2), 1.51 (m, 8H, NCH_2CH_2). $^{13}\text{C}\{^1\text{H}\}$ NMR (101 MHz, C_6D_6 , 298 K): δ 49.4 (br, NCH_2CH_2), 26.6 (br, NCH_2CH_2).

NMR data in CD_2Cl_2 :

^{11}B NMR (160 MHz, CD_2Cl_2 , 298 K): δ 26.3 (d, $^1J_{\text{B,H}} = 127$ Hz). $^1\text{H}\{^{11}\text{B}\}$ NMR (300 MHz, CD_2Cl_2 , 298 K): δ 3.93 (s, 1H, BH), 3.27 (m, 8H, NCH_2CH_2), 1.67 (m, 8H, NCH_2CH_2).

Diaminoborane $(\text{N}^t\text{BuH})(\text{NEt}_2)\text{BH}$. The general procedure described in section 2.3 using $\text{N}^t\text{BuH}_2\cdot\text{BH}_3$ and NEt_2H was followed leading to 85 mg (99% yield) of diaminoboranes $(\text{N}^t\text{BuH})(\text{NEt}_2)\text{BH}$ (96%) and $(\text{N}^t\text{BuH})_2\text{BH}$ (4%) (by ^1H NMR spectroscopy).

NMR data in C_6D_6 :

^{11}B NMR (160 MHz, C_6D_6 , 298 K): δ 26.9 (d, $^1J_{\text{B,H}} = 127$ Hz). $^1\text{H}\{^{11}\text{B}\}$ NMR (400 MHz, C_6D_6 , 298 K): δ 4.32 (d, $J_{\text{H,H}} = 8.8$ Hz, 1H, BH), 3.15-2.67 (br, 4H, NCH_2CH_3), 2.64 (br, 1H, NH), 1.19 (s, 9H, ^tBu), 0.96 (br t, 6H, $J_{\text{H,H}} = 6.0$ Hz, NCH_2CH_3). $^{13}\text{C}\{^1\text{H}\}$

NMR (101 MHz, C₆D₆, 298 K): δ 48.5 (s, C(CH₃)₃), 46.8 and 36.5 (br, NCH₂CH₃), 33.5 (s, C(CH₃)₃), 16.9 and 15.9 (br, NCH₂CH₃).

NMR data in CD₂Cl₂:

¹¹B NMR (160 MHz, CD₂Cl₂, 298 K): δ 26.7 (d, ¹J_{B,H} = 127 Hz). ¹H{¹¹B} NMR (400 MHz, C₆D₆, 298 K): δ 3.96 (d, J_{H,H} = 9.5 Hz, 1H, BH), 2.90 (br, 4H, NCH₂CH₃), 2.70 (br, 1H, NH), 1.16 (s, 9H, ^tBu), 1.01 (t, 6H, J_{H,H} = 7.1 Hz, NCH₂CH₃). ¹³C{¹H} NMR (101 MHz, C₆D₆, 298 K): δ 48.6 (s, C(CH₃)₃), 33.5 (s, C(CH₃)₃), 16.2 (br, NCH₂CH₃) (the signals for the NCH₂ fragments are too broad and are lost in the baseline).

Diaminoborane (N^tBuH)(NMe₂)BH. The general procedure described in section 2.3 using NMe₂H·BH₃ and N^tBuH₂ was followed leading to 54 mg of diaminoboranes (N^tBuH)(NMe₂)BH (86%), (N^tBuH)₂BH (6%), (NMe₂)₂BH (2%) (aprox. yield 71% sum of all), cyclic aminoboranes [NMe₂BH₂]₂ (5%) and another unidentified species at δ 2.16 (1%). The ¹¹B NMR of the crude reaction mixture in CD₂Cl₂ before workup reveals the presence of (N^tBuH)(NMe₂)BH, (NMe₂)₂BH and (N^tBuH)₂BH (ca. 78.4 % of all diaminoboranes), cyclic aminoboranes [NMe₂BH₂]₂ (δ 5.2; 3%) and [N^tBuHBH₂]₃ (δ -5.2, ¹J_{B,H} ~ 110Hz) (ca. 4.3 %), and another species that has been tentatively identified as Me₂NHBH₂NMe₂BH₃ (δ 2.1 [t, ¹J_{B,H} ~ 110 Hz, BH₂], δ -13.6 [q, ¹J_{B,H} ~ 93 Hz, BH₃]) (ca 5%).

NMR data in C₆D₆:

¹¹B NMR (128 MHz, C₆D₆, 298 K): δ 27.3 (d, ¹J_{B,H} = 129 Hz). ¹H{¹¹B} NMR (400 MHz, C₆D₆, 298 K): δ 4.30 (d, J_{H,H} = 9.4 Hz, 1H, BH), 2.10-2.80 (br, 7H, NCH₃ and NH), 1.18 (s, 9H, ^tBu). ¹³C{¹H} NMR (101 MHz, C₆D₆, 298 K): δ 48.8 (s, C(CH₃)₃), 42.9 and 35.5 (br, NCH₃), 33.5 (s, C(CH₃)₃).

NMR data in CD₂Cl₂:

¹¹B NMR (128 MHz, CD₂Cl₂, 298 K): δ 26.9 (d, ¹J_{B,H} = 129 Hz). ¹H{¹¹B} NMR (300 MHz, C₆D₆, 298 K): δ 3.93 (d, J_{H,H} = 9.4 Hz, 1H, BH), 2.40-2.80 (br, 7H, NCH₃ and NH), 1.16 (s, 9H, ^tBu).

Diaminoborane (N^tBuH)[N(CH₂)₄]BH.

The general procedure described in section 2.3 using N^tBuH₂·BH₃ and HN(CH₂)₄ was followed leading to 58 mg of diaminoboranes (N^tBuH)[N(CH₂)₄]BH (92%), (N^tBuH)₂BH (8%) (aprox. yield 68% sum of both). The ¹¹B NMR of the crude reaction mixture in CD₂Cl₂ reveals the presence of (N^tBuH)[N(CH₂)₄]BH and (N^tBuH)₂BH (ca.

94 %), and other unidentified species at δ 3.2, 1.4 and 2.1 (sum of integrals constitute 4% of the total amount), together with some $\text{N}(\text{CH}_2)_4\text{HBH}_2\text{N}(\text{CH}_2)_4\text{BH}_3$ (δ 0.1 (t, $^1J_{\text{B,H}} \sim 112$ Hz, BH_2), δ -15.2 (q, $^1J_{\text{B,H}} \sim 93$ Hz, BH_3); ca. 4%).

NMR data in C_6D_6 :

^{11}B NMR (128 MHz, C_6D_6 , 298 K): δ 25.9 (d, $^1J_{\text{B,H}} = 127$ Hz). $^1\text{H}\{^{11}\text{B}\}$ NMR (400 MHz, C_6D_6 , 298 K): δ 4.54 (d, $J_{\text{H,H}} = 9.4$ Hz, 1H, BH), 3.24 and 2.80 (br, 2H each, NCH_2CH_2), 2.68 (br, 1H, NH), 1.50 (br, 4H, NCH_2CH_2), 1.22 (s, 9H, ^tBu). $^{13}\text{C}\{^1\text{H}\}$ NMR (101 MHz, C_6D_6 , 298 K): δ 50.7 (br, NCH_2CH_2), 48.6 (s, $\text{C}(\text{CH}_3)_3$), 44.5 (br, NCH_2CH_2), 33.6 (s, $\text{C}(\text{CH}_3)_3$), 26.5 (br, NCH_2CH_2).

NMR data in CD_2Cl_2 :

^{11}B NMR (128 MHz, CD_2Cl_2 , 298 K): δ 25.6 (d, $^1J_{\text{B,H}} = 127$ Hz). $^1\text{H}\{^{11}\text{B}\}$ NMR (300 MHz, C_6D_6 , 298 K): δ 4.10 (d, $J_{\text{H,H}} = 9.4$ Hz, 1H, BH), 32.83-3.36 (br, 4H, NCH_2CH_2), 2.73 (br, 1H, NH), 1.72 (br, 4H, NCH_2CH_2), 1.17 (s, 9H, ^tBu).

2.5 Synthesis of amine-borane adduct $[\text{Pt}(\text{I}^t\text{Bu}')(\text{I}^t\text{Bu})(\text{H}_3\text{B}\cdot\text{N}^t\text{BuH}_2)][\text{BAr}^F]$ 3b.

A mixture of complex **1** (25 mg, 0.017 mmol) and the corresponding amine-borane $\text{N}^t\text{BuH}_2\cdot\text{BH}_3$ (1.5 mg, 0.017 mmol) is dissolved in 0.5 mL of CD_2Cl_2 cooled to -30 °C. The sample is brought to the spectrometer and characterized by multinuclear NMR at 0 °C.

^1H NMR (500 MHz, CD_2Cl_2 , 0 °C): δ 7.72 (br, 8H, $o\text{-H}(\text{Ar}^F)$), 7.56 (br, 4H, $p\text{-H}(\text{Ar}^F)$), 7.29 (s, 2H, =CH), 7.11 (d, $^3J_{\text{H,H}} = 2.3$ Hz, =CH), 6.88 (d, $^3J_{\text{H,H}} = 2.3$ Hz, =CH), 3.10 (br s, 2H, NH_2), 2.37 (s+d, $^3J_{\text{Pt,H}} = 90$ Hz, 2H, Pt- CH_2), 1.93 (s, 18H, $\text{C}(\text{CH}_3)_3$, I^tBu), 1.67 (s, 9H, $\text{C}(\text{CH}_3)_3$, $\text{I}^t\text{Bu}'$), 1.45 (s, 6H, $\text{C}(\text{CH}_2)(\text{CH}_3)_2$), 1.19 (s, 9H, $\text{NH}_2\text{C}(\text{CH}_3)_3$), 0.12 (br s, 3H, BH_3).

$^{11}\text{B}\{^1\text{H}\}$ NMR (128 MHz, CD_2Cl_2 , 0 °C): δ -6.7 ($\text{B}(\text{Ar}^F)_4$), -18.2 (br).

$^{13}\text{C}\{^1\text{H}\}$ NMR (126 MHz, CD_2Cl_2 , 0 °C): δ 173.8 (C=Pt, I^tBu), 167.5 (C=Pt, $\text{I}^t\text{Bu}'$), 162.1 (q, $J_{\text{C,B}} = 49.5$ Hz, *ipso*-C (Ar^F), 135.1 (*o*-C (Ar^F)), 129.1 (q, $J_{\text{C,F}} = 36.8, 32.4$ Hz, *m*-C (Ar^F)), 124.9 (q, $J_{\text{C,F}} = 272.5$, CF_3 , (Ar^F)), 119.6 (=CH, I^tBu), 118.3 and 114.7 (=CH, $\text{I}^t\text{Bu}'$), 117.9 (*p*-C(Ar^F)), 64.7 ($\text{C}(\text{CH}_2)(\text{CH}_3)_2$), 60.2 ($\text{C}(\text{CH}_3)_3$, I^tBu), 58.1 ($\text{C}(\text{CH}_3)_3$, $\text{I}^t\text{Bu}'$), 55.1 ($\text{NH}_2\text{C}(\text{CH}_3)_3$), 32.3 ($\text{C}(\text{CH}_3)_3$, I^tBu), 31.1 ($\text{C}(\text{CH}_3)_3$, $\text{I}^t\text{Bu}'$), 30.6 ($\text{C}(\text{CH}_2)(\text{CH}_3)_2$), 28.2 ($\text{NH}_2\text{C}(\text{CH}_3)_3$), 20.7 ($\text{CH}_2\text{-Pt}$).

2.6 Synthesis of pyridine-borane adduct 3c. C₅H₅N·BH₃ (4 μL, 0.039 mmol) is added, at rt to a solution of complex **1** (55 mg, 0.039 mmol) in 1 ml of CH₂Cl₂ (or CD₂Cl₂). A rapid color change is observed from bright orange to almost colorless. According to NMR spectroscopy full conversion of **1** into **3c** is observed. The solvent is removed under vacuum and the off-white solid is washed with pentane (2 x 5mL). Drying under vacuum leads to an off-white complex (50 mg, 86% yield). Crystals suitable for X-ray diffraction studies were grown by slow diffusion of a concentration solution of **3c** in dichloromethane into pentane at 0 °C. Complex **3c** is unstable in CH₂Cl₂ solutions for prolonged periods of time, but can be stored under argon in the solid state without significant degradation.

¹H{¹¹B} NMR (400 MHz, CD₂Cl₂, 25 °C): δ 8.35 (d, 2H, ³J_{HH} = 5.3 Hz, CHpy), 8.01 (t, 1H, ³J_{HH} = 7.6 Hz, CHpy), 7.74 (br, 8H, *o*-H(Ar^F)), 7.58 (br, 4H, *p*-H(Ar^F)), 7.56 (d, 2H, ³J_{HH} = 7.1 Hz, CHpy), 7.24 (s, 2H, =CH), 7.09 (d, ³J_{H,H} = 2.1 Hz, =CH), 6.88 (d, ³J_{H,H} = 2.1 Hz, =CH), 2.36 (s+d, ³J_{Pt,H} = 90 Hz, 2H, Pt-CH₂), 1.89 (s, 18H, C(CH₃)₃, I'Bu'), 1.53 (s, 9H, C(CH₃)₃, I'Bu'), 1.47 (s, 6H, C(CH₂)(CH₃)₂), 1.37 (br s, 3H, BH₃).

¹¹B{¹H} NMR (128 MHz, CD₂Cl₂, 0 °C): δ -6.6 (B(Ar^F)₄), -8.9 (br).

¹³C{¹H} NMR (126 MHz, CD₂Cl₂, 0 °C): δ 171.6 (C=Pt, I'Bu'), 166.5 (C=Pt, I'Bu'), 162.1 (q, J_{C,B} = 49.5 Hz, *ipso*-C (Ar^F)), 148.1 (CH_{py}), 141.5 (CH_{py}), 135.1 (*o*-C (Ar^F)), 129.1 (q, J_{CF} = 36.8, 32.4 Hz, *m*-C (Ar^F)), 126.4 (CH_{py}), 124.9 (q, J_{C,F} = 272.5, CF₃, (Ar^F)), 119.5 (=CH, I'Bu'), 118.4 and 113.6 (=CH, I'Bu'), 117.9 (*p*-C(Ar^F)), 64.7 (br, C(CH₂)(CH₃)₂), 59.9.2 (C(CH₃)₃, I'Bu'), 57.9 (C(CH₃)₃, I'Bu'), 32.5 (C(CH₃)₃, I'Bu'), 30.9 (C(CH₃)₃, I'Bu'), 30.6 (C(CH₂)(CH₃)₂), 28.2 (NH₂C(CH₃)₃), 19.6 (CH₂-Pt).

Elemental analyses calcd (%) for C₅₉H₅₉B₂F₂₄N₅Pt: C, 46.90; H, 3.94; N, 4.64;
Found: C, 46.73; H, 4.15; N, 4.28.

3. NMR SPECTRA OF DIAMINOBORANES

3.1 Diaminoborane ($N^t\text{BuH}$)₂BH.

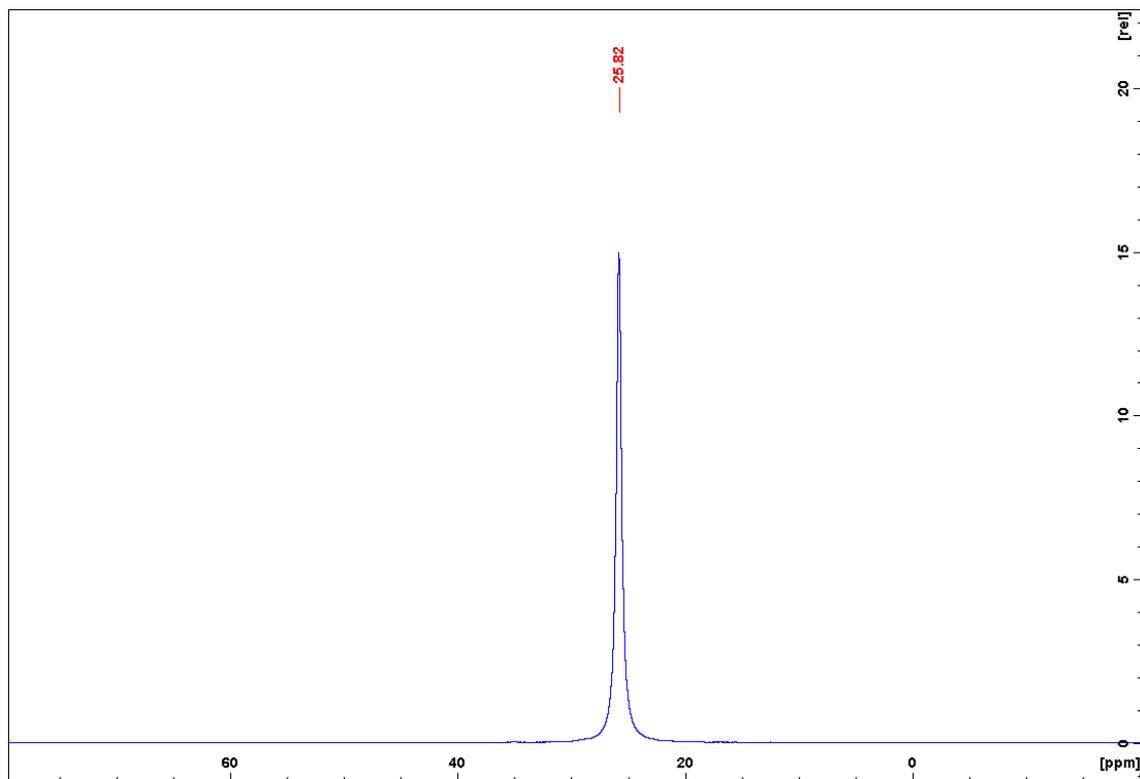


Figure S2. $^{11}\text{B}\{^1\text{H}\}$ NMR of $(N^t\text{BuH})_2\text{BH}$ in C_6D_6 .

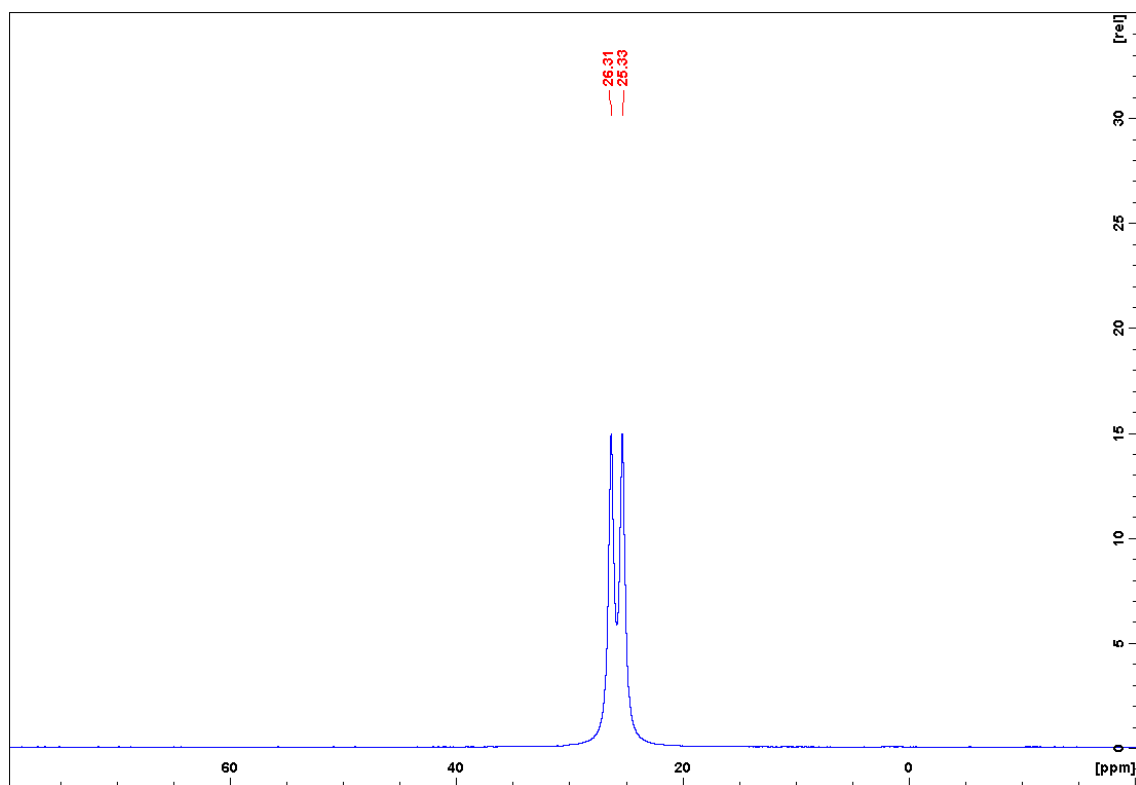


Figure S3. ^{11}B NMR of $(N^t\text{BuH})_2\text{BH}$ in C_6D_6 .

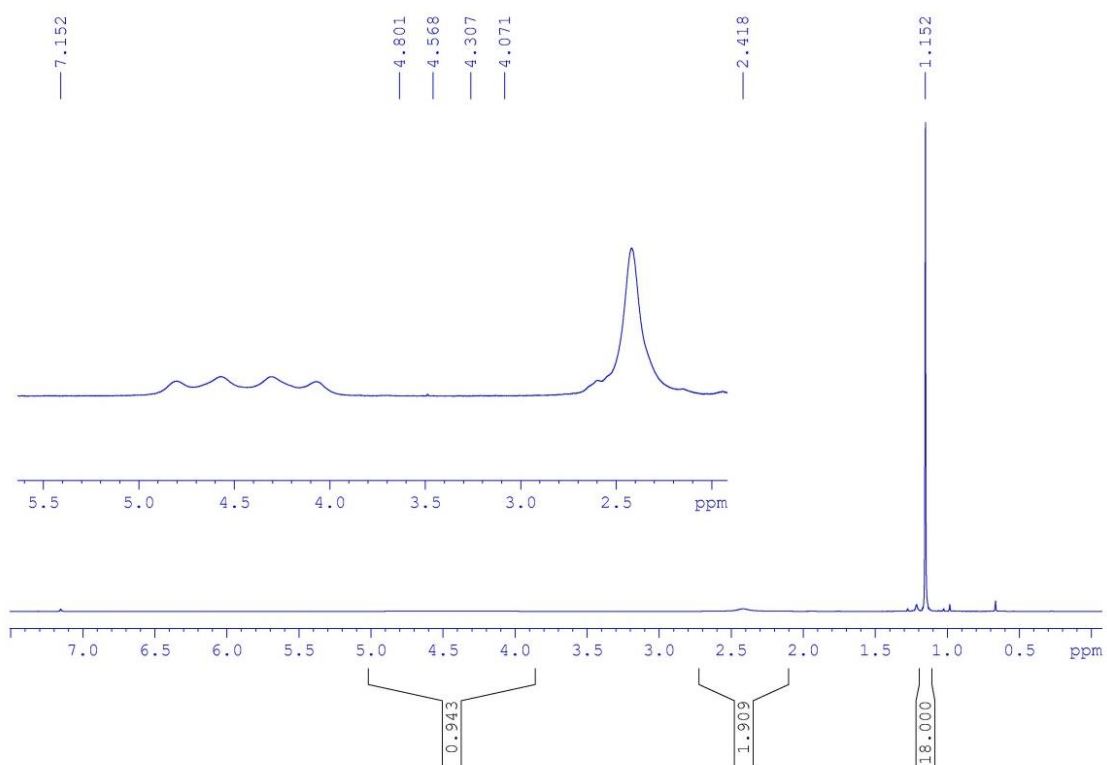


Figure S4. ^1H NMR of $(\text{N}^t\text{BuH})_2\text{BH}$ in C_6D_6 .

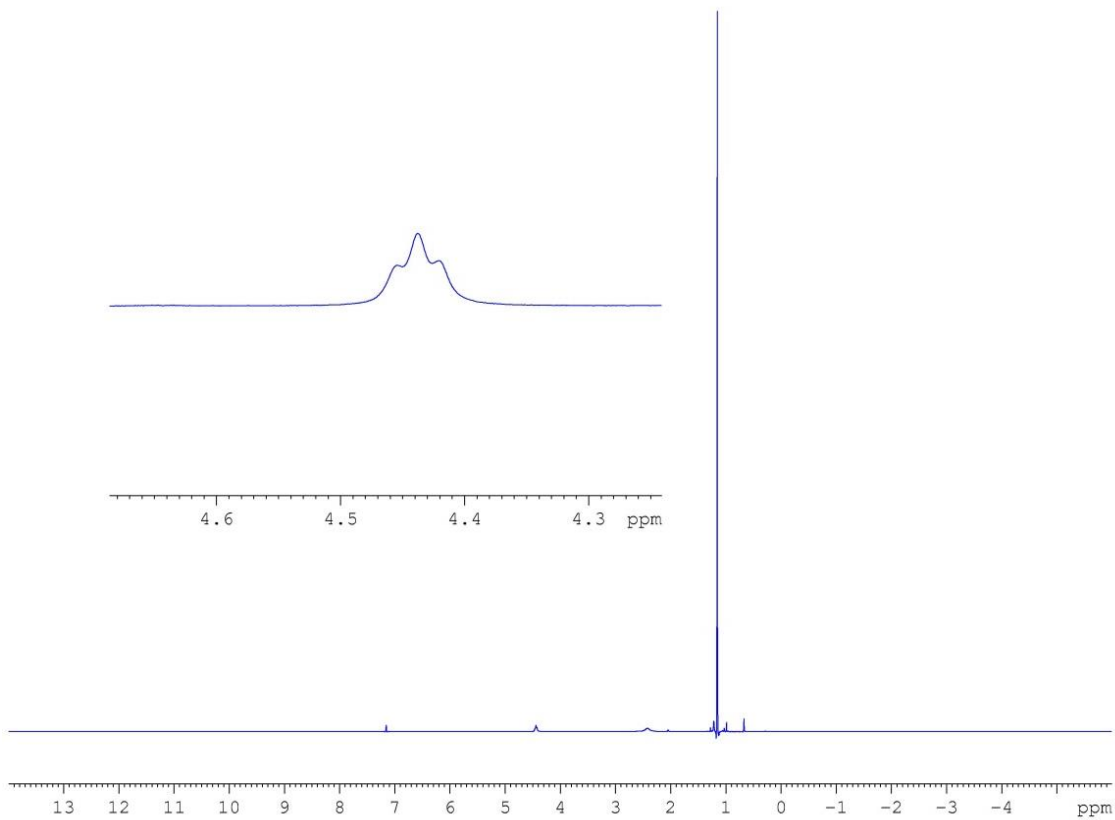


Figure S5. $^1\text{H}\{^{11}\text{B}\}$ NMR of $(\text{N}^t\text{BuH})_2\text{BH}$ in C_6D_6 .

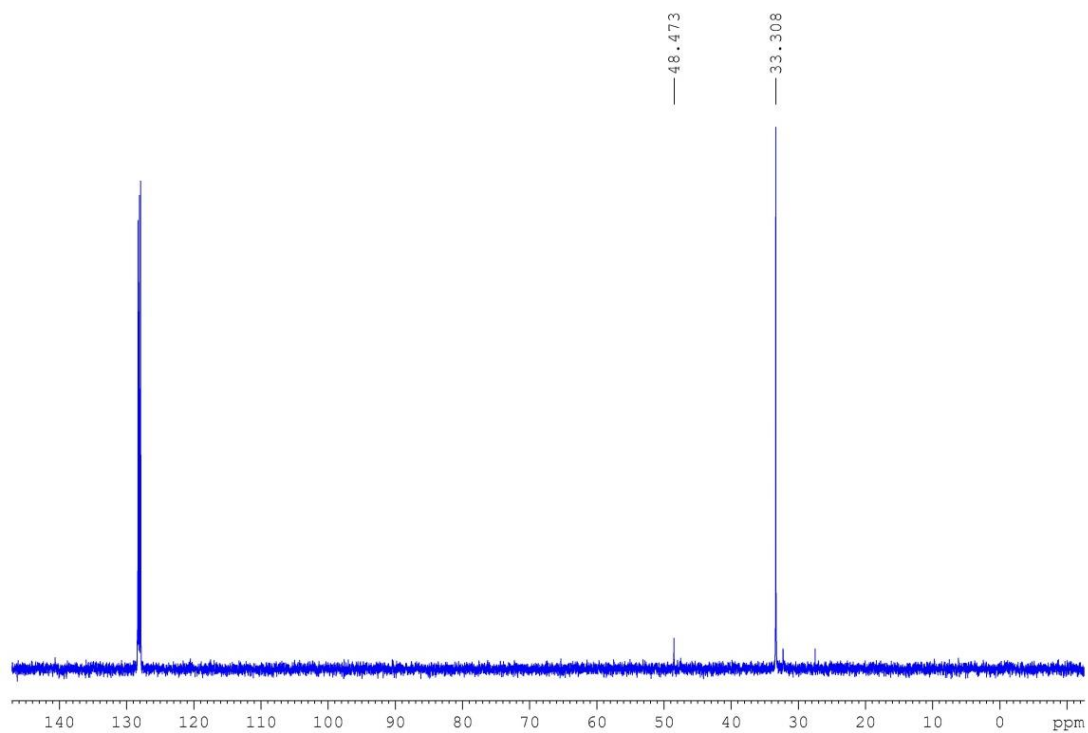


Figure S6. $^{13}\text{C}\{^1\text{H}\}$ NMR of $(\text{N}^t\text{BuH})_2\text{BH}$ in C_6D_6 .

3.2 Diaminoborane $(\text{NEt}_2)_2\text{BH}$.

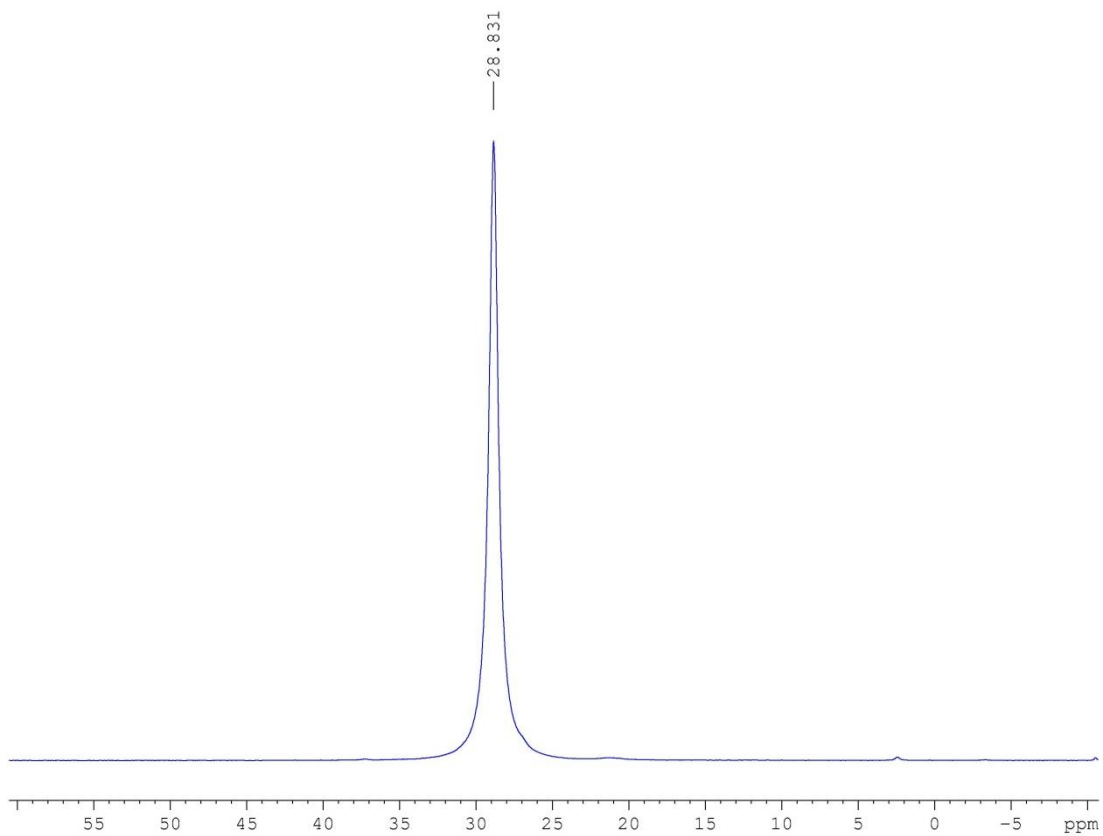


Figure S7. $^{11}\text{B}\{^1\text{H}\}$ NMR of $(\text{NEt}_2)_2\text{BH}$ in C_6D_6 .

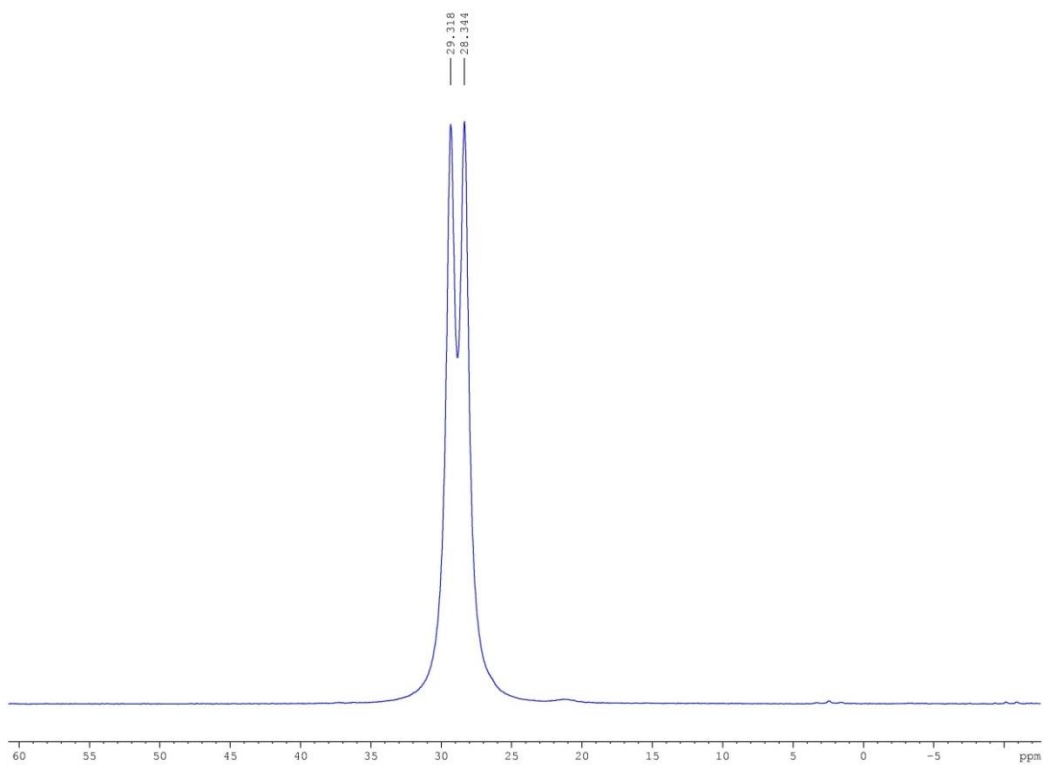


Figure S8. ^{11}B NMR of $(\text{NEt}_2)_2\text{BH}$ in C_6D_6 .

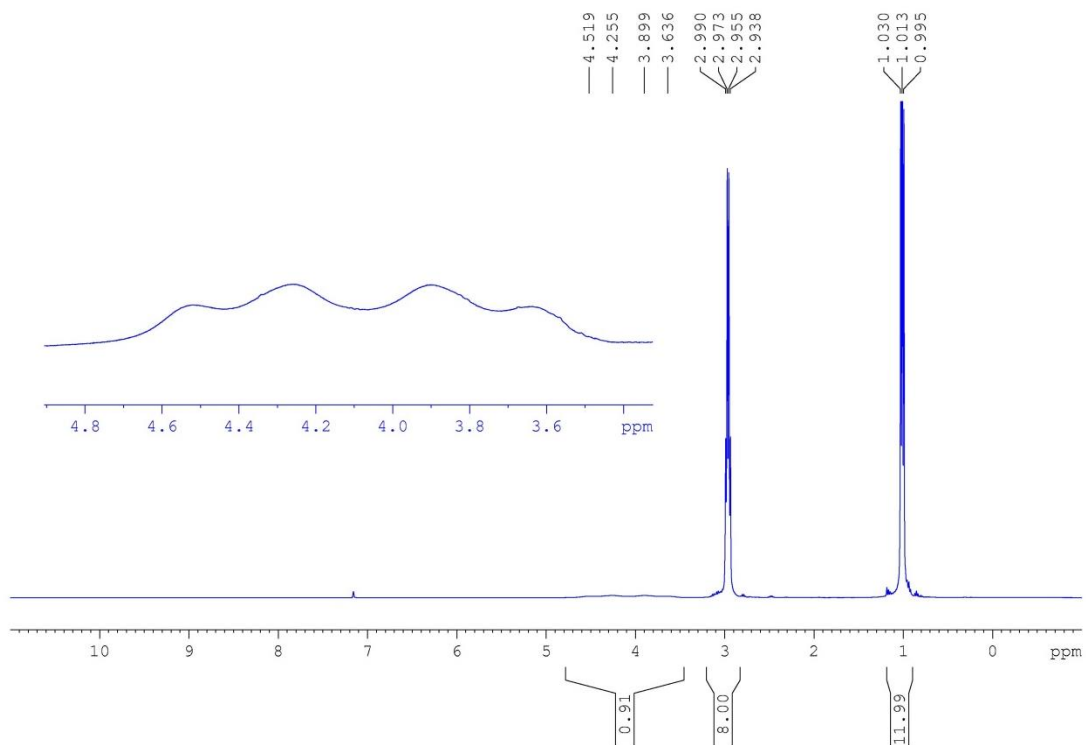


Figure S9. ^1H NMR of $(\text{NEt}_2)_2\text{BH}$ in C_6D_6 .

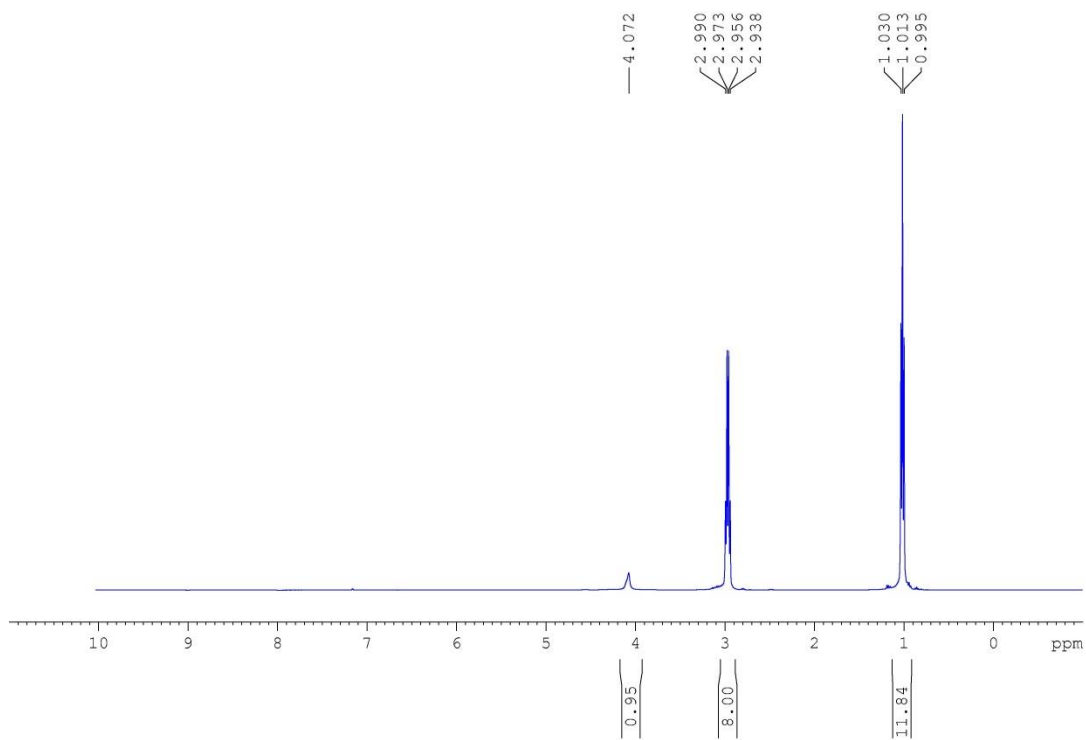


Figure S10. $^1\text{H}\{^{11}\text{B}\}$ NMR of $(\text{NEt}_2)_2\text{BH}$ in C_6D_6 .

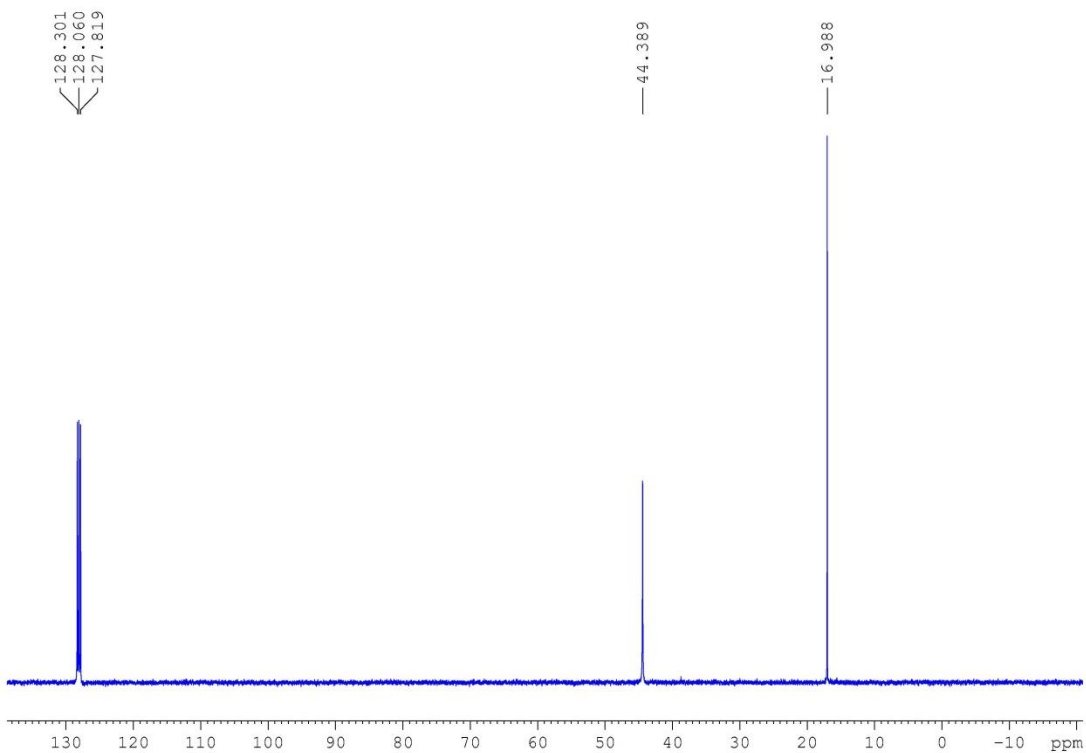


Figure S11. $^{13}\text{C}\{^1\text{H}\}$ NMR of $(\text{NEt}_2)_2\text{BH}$ in C_6D_6 .

3.3 Diaminoborane $[\text{N}(\text{CH}_2)_4]_2\text{BH}$.

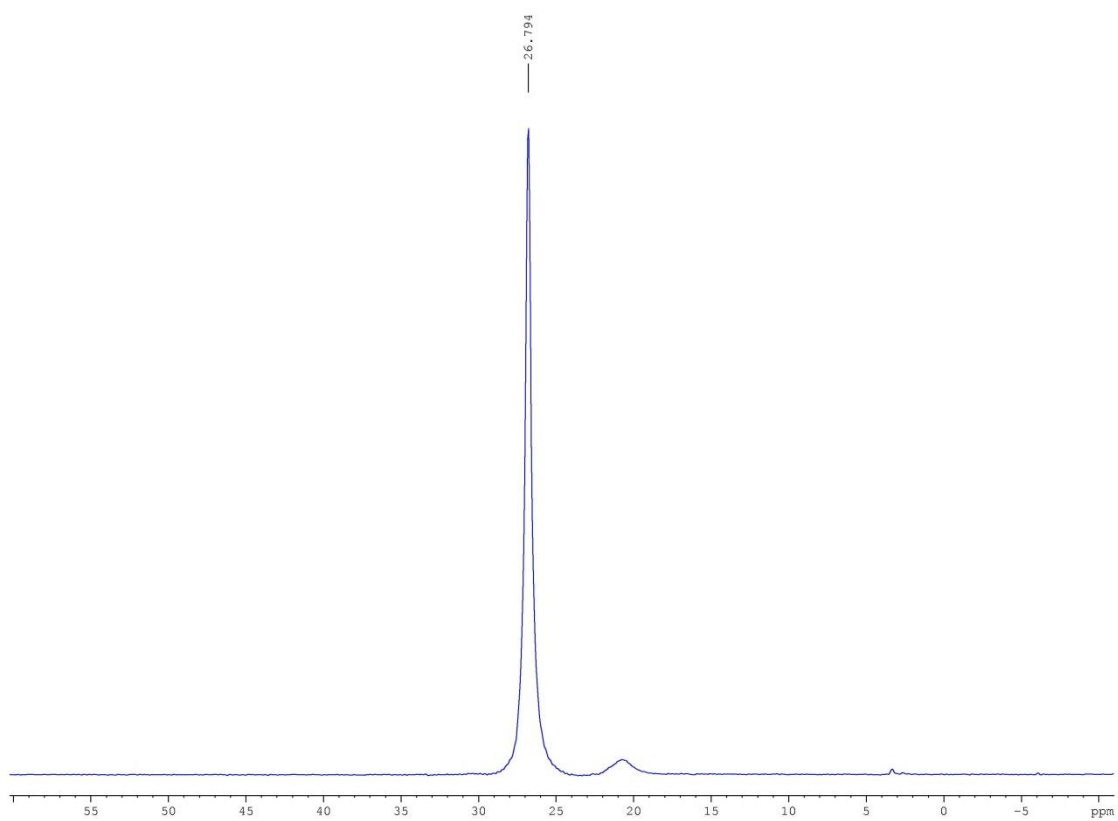


Figure S12. $^{11}\text{B}\{^1\text{H}\}$ NMR of $[\text{N}(\text{CH}_2)_4]_2\text{BH}$ in C_6D_6 .

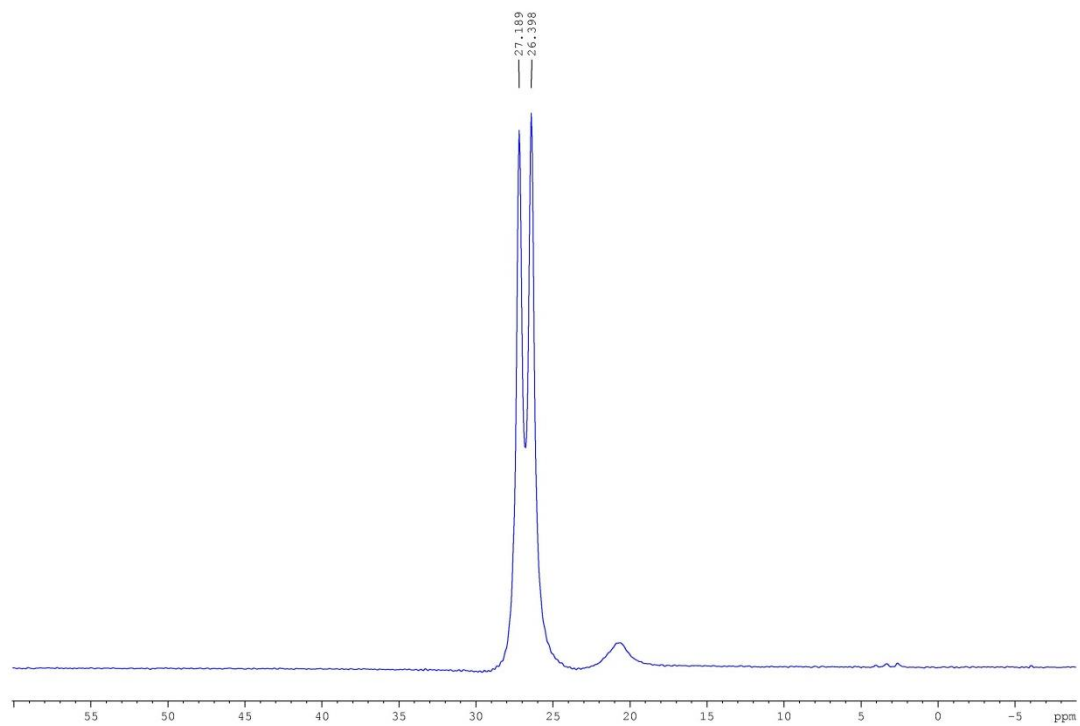


Figure S13. ^{11}B NMR of $[\text{N}(\text{CH}_2)_4]_2\text{BH}$ in C_6D_6 .

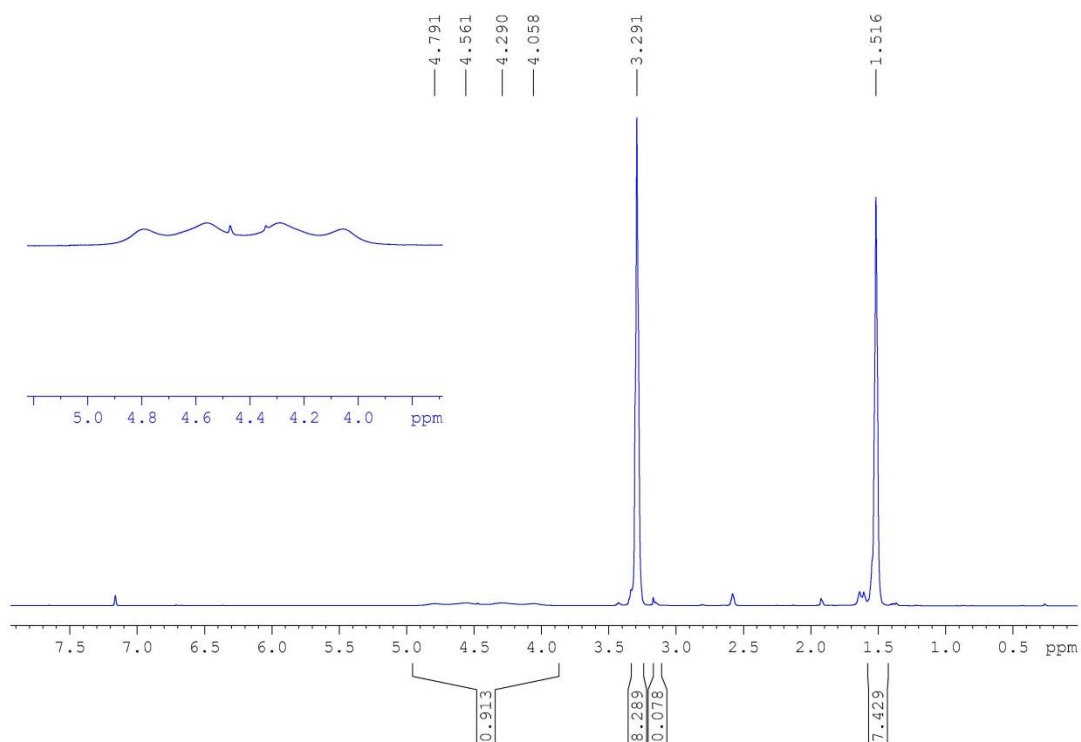


Figure S14. ^1H NMR of $[\text{N}(\text{CH}_2)_4]_2\text{BH}$ in C_6D_6 .

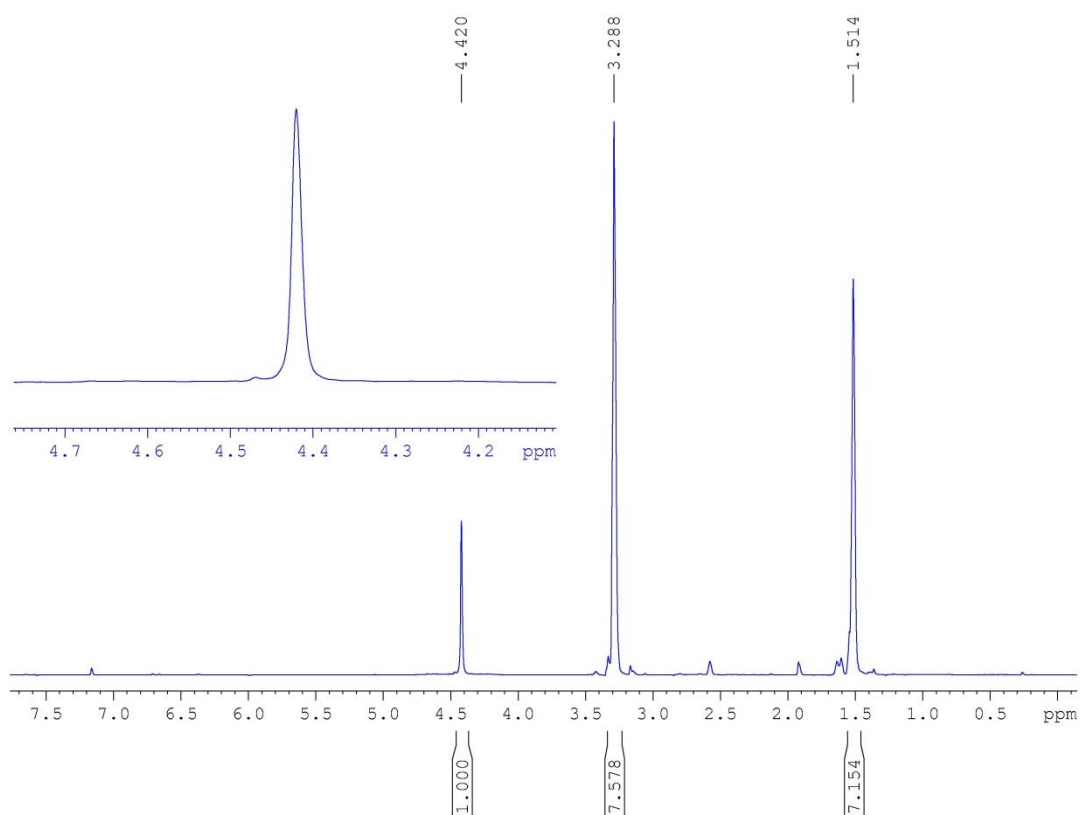


Figure S15. $^1\text{H}\{^{11}\text{B}\}$ NMR of $[\text{N}(\text{CH}_2)_4]_2\text{BH}$ in C_6D_6 .

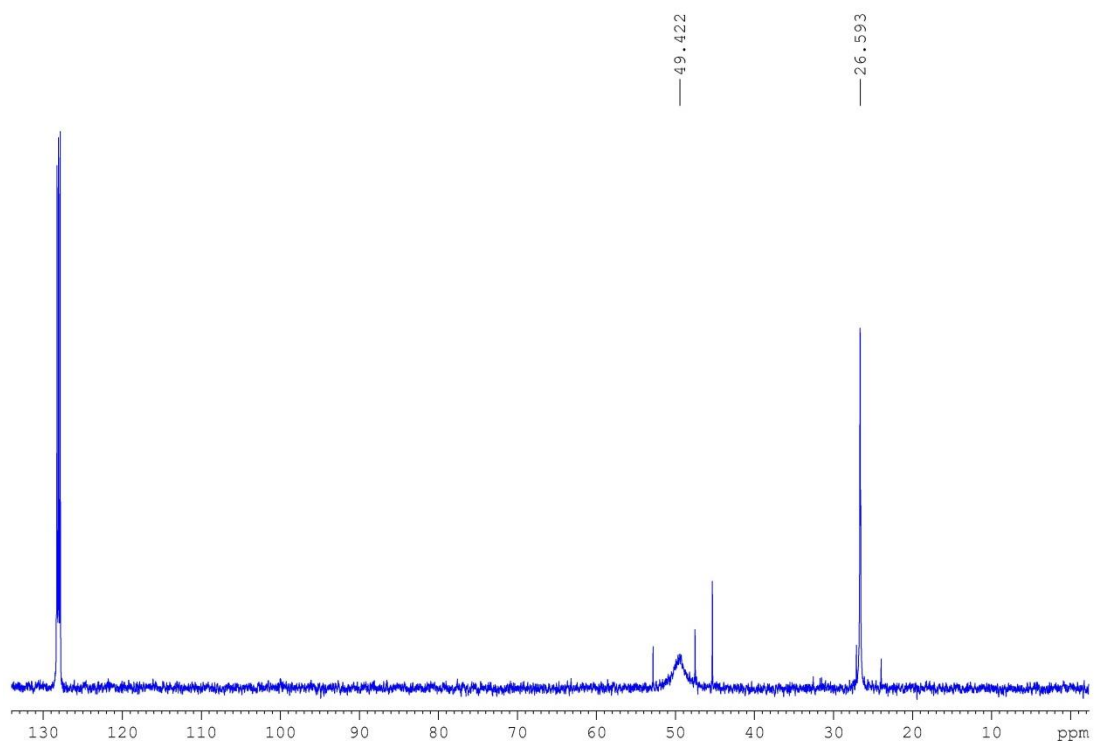


Figure S16. $^{13}\text{C}\{^1\text{H}\}$ NMR of $[\text{N}(\text{CH}_2)_4]_2\text{BH}$ in C_6D_6 .

3.4 Diaminoborane (N^tBuH)(NEt_2)BH.

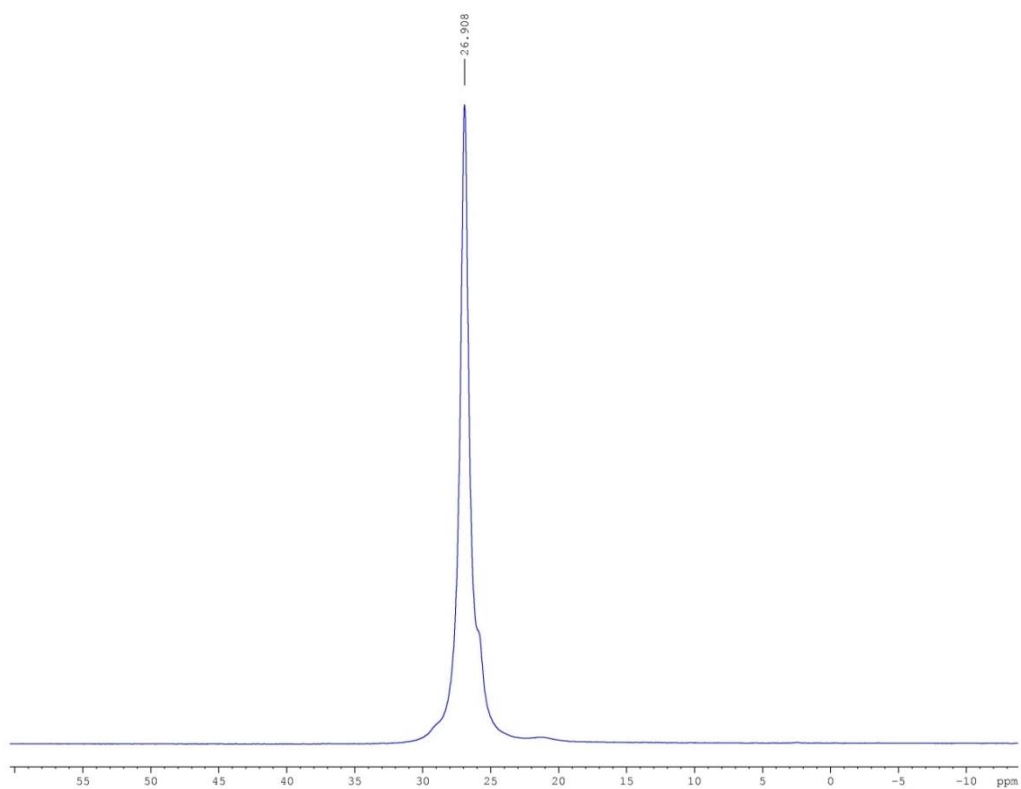


Figure S17. $^{11}\text{B}\{^1\text{H}\}$ NMR of $(\text{N}^t\text{BuH})(\text{NEt}_2)\text{BH}$ in C_6D_6 .

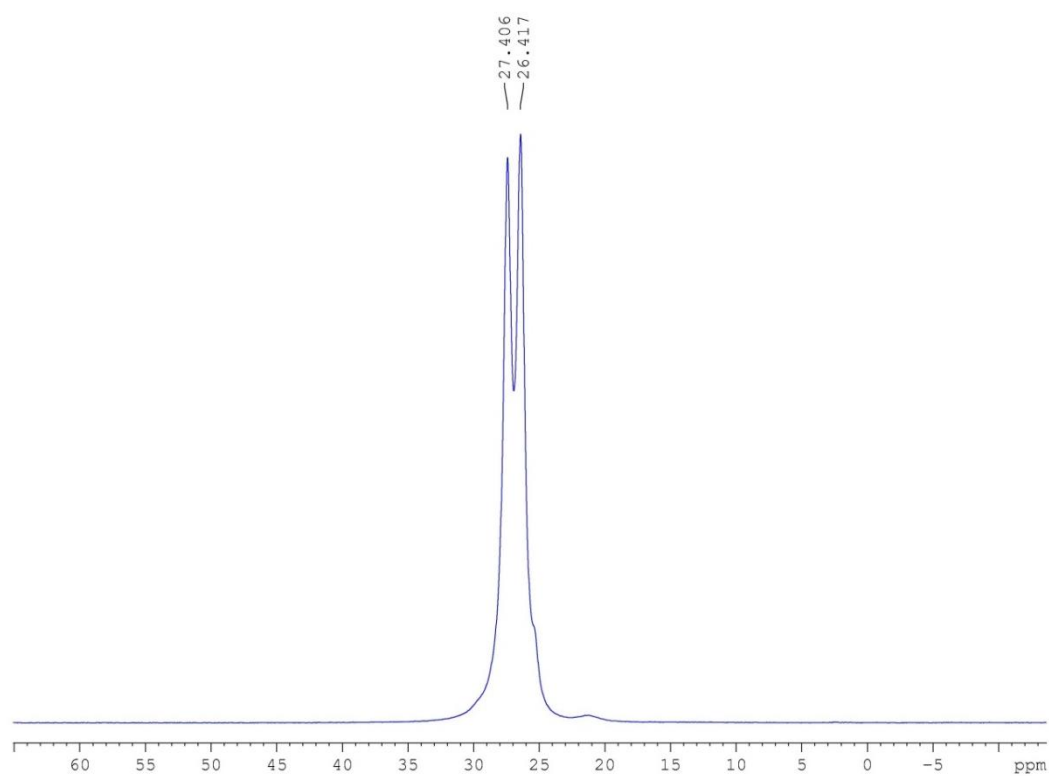


Figure S18. ^{11}B NMR of $(\text{N}^t\text{BuH})(\text{NEt}_2)\text{BH}$ in C_6D_6 .

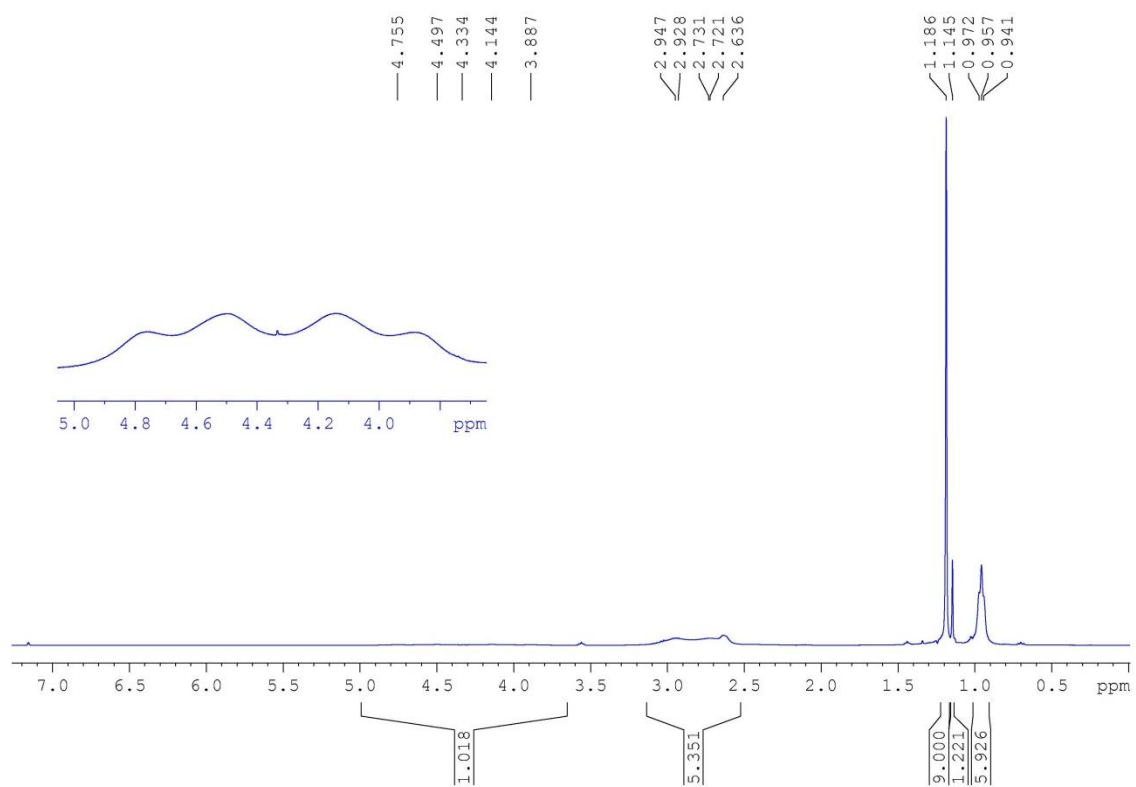


Figure S19. ^1H NMR of $(\text{N}^t\text{BuH})(\text{NEt}_2)\text{BH}$ in C_6D_6 .

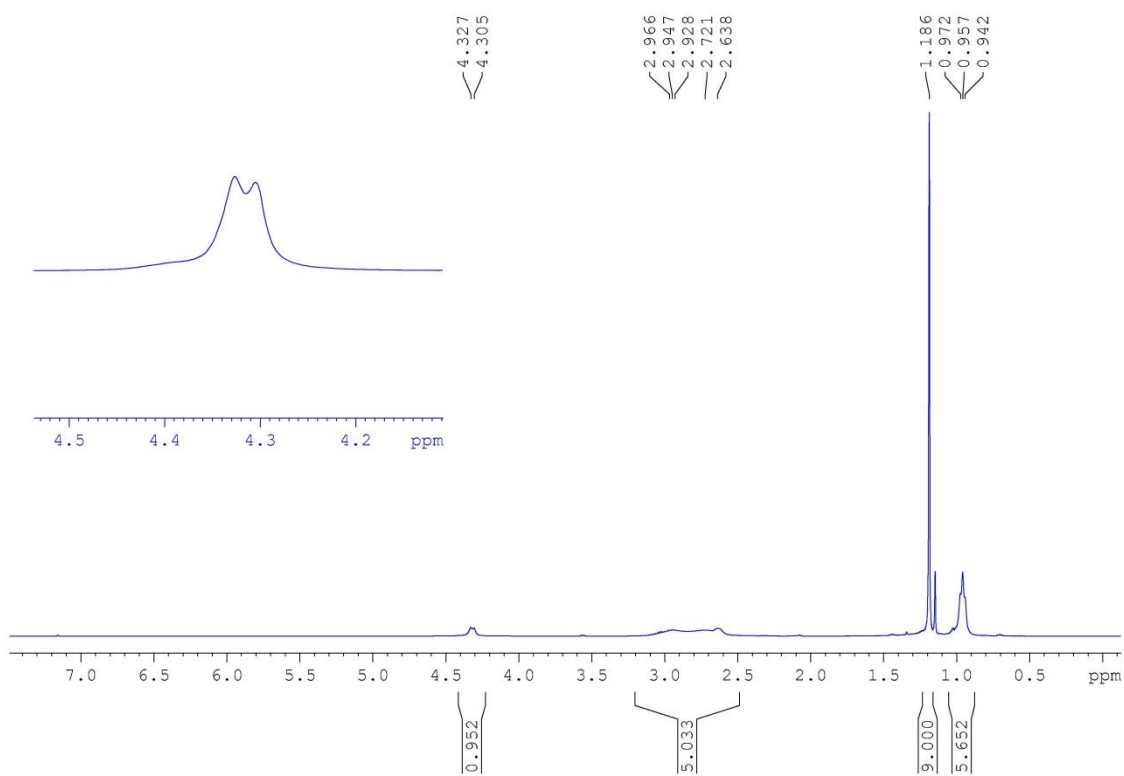


Figure S20. $^1\text{H}\{^{11}\text{B}\}$ NMR of $(\text{N}^t\text{BuH})(\text{NEt}_2)\text{BH}$ in C_6D_6 .

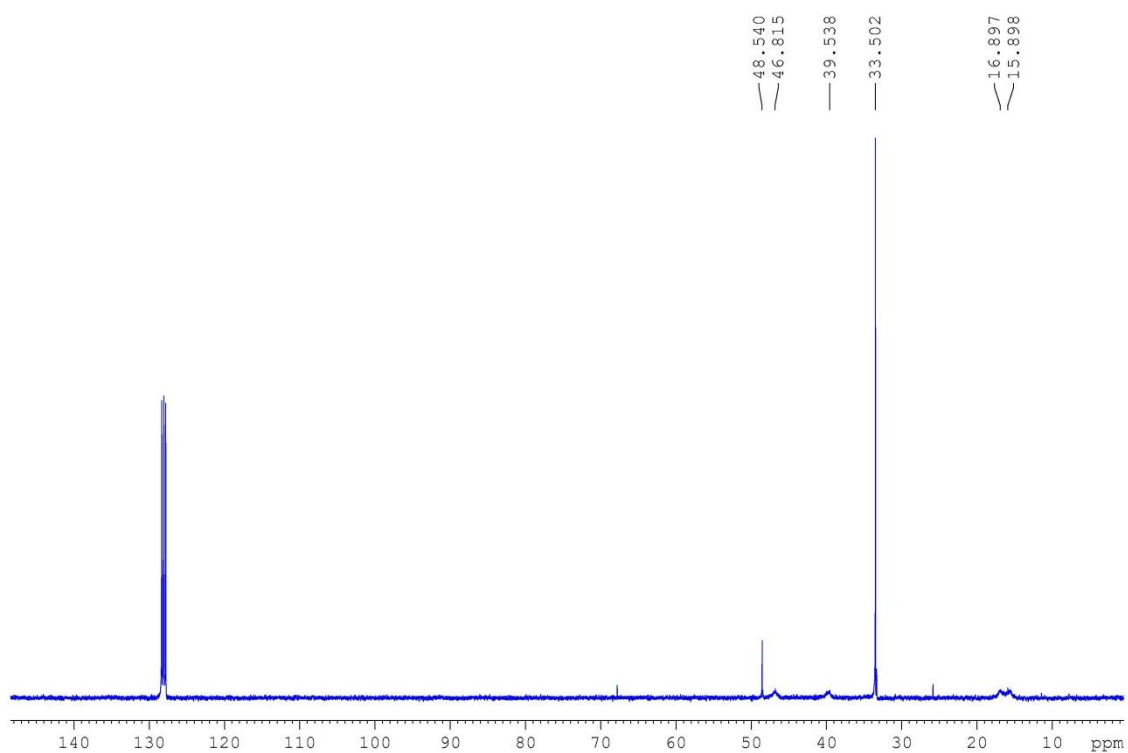


Figure S21. $^{13}\text{C}\{^1\text{H}\}$ NMR of $(\text{N}^t\text{BuH})(\text{NEt}_2)\text{BH}$ in C_6D_6 .

3.5 Diaminoborane (N^tBuH)(NMe_2)BH.

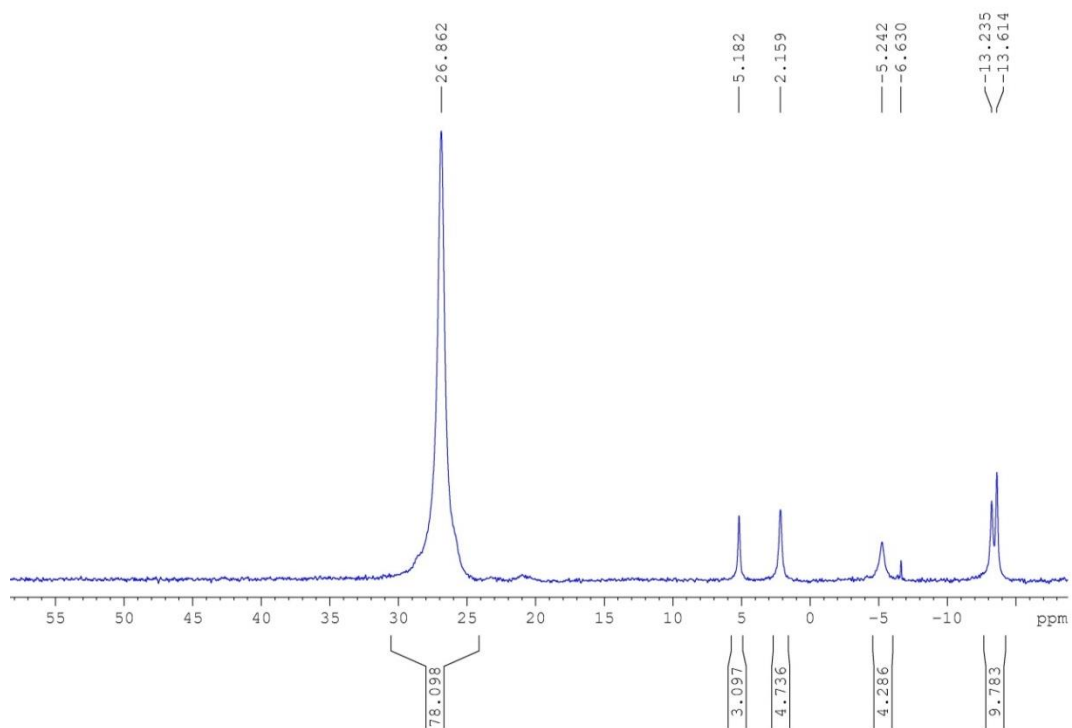


Figure S22. $^{11}B\{^1H\}$ NMR of the crude reaction mixture of $NMe_2H \cdot BH_3$ and N^tBuH_2 in CD_2Cl_2 .

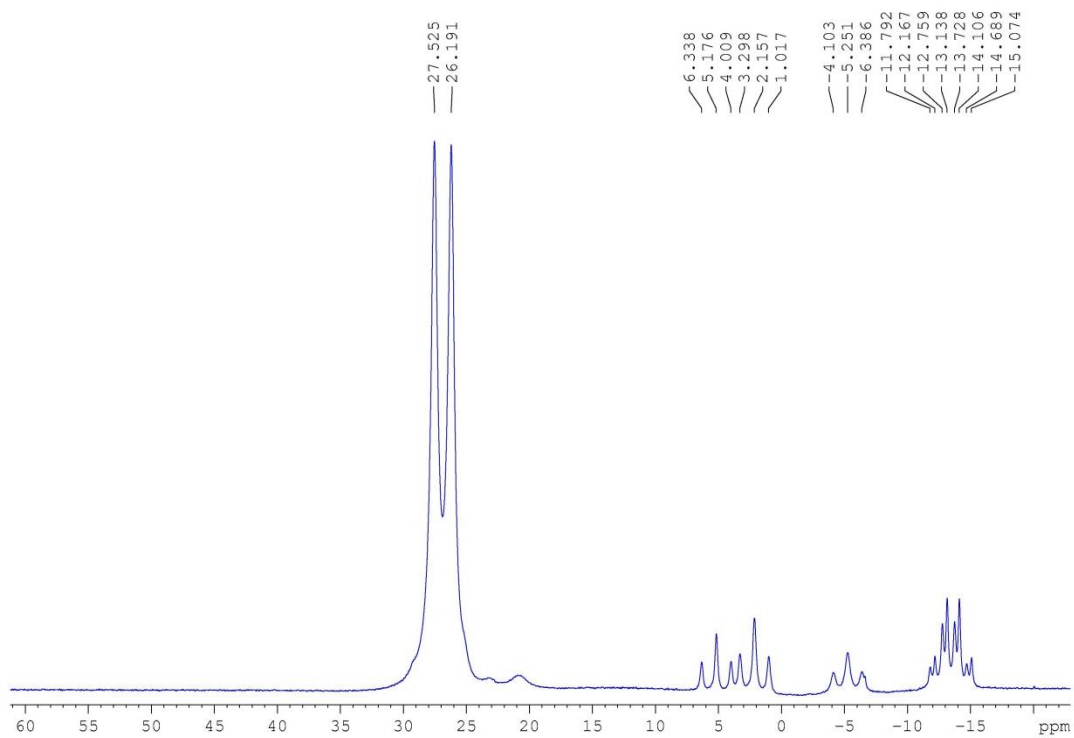


Figure S23. ^{11}B NMR of the crude reaction mixture of $NMe_2H \cdot BH_3$ and N^tBuH_2 in CD_2Cl_2 .

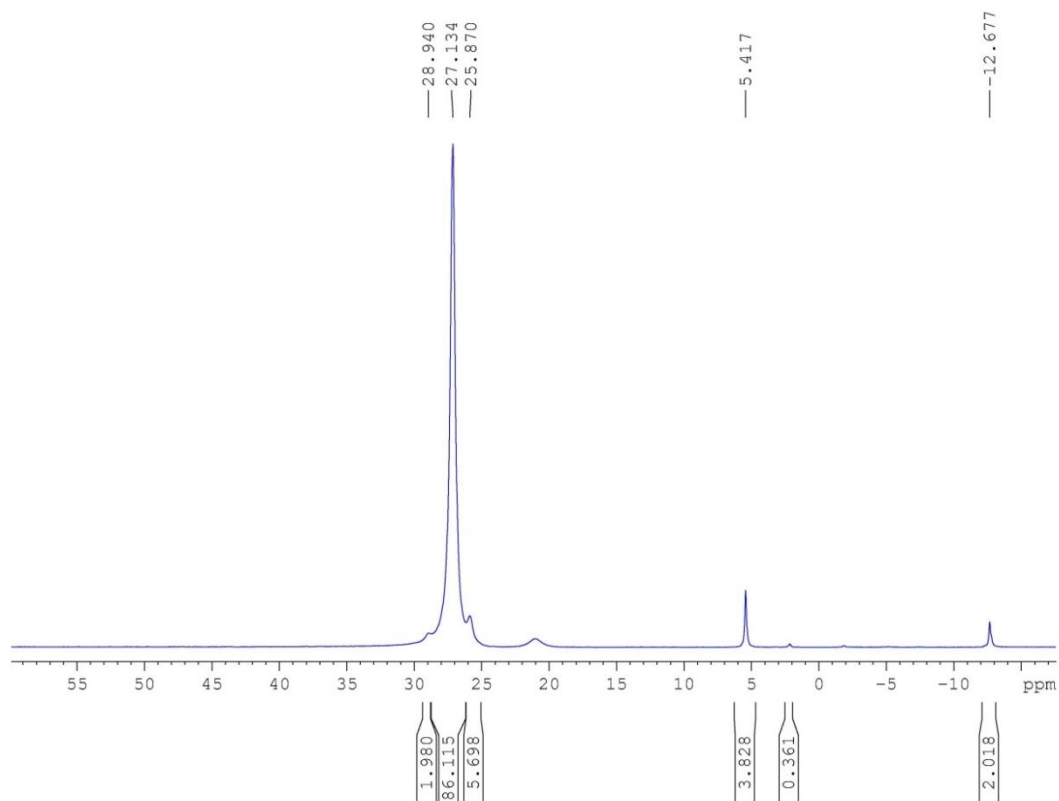


Figure S24. $^{11}\text{B}\{^1\text{H}\}$ NMR of the reaction of $\text{NMe}_2\text{H}\cdot\text{BH}_3$ and N^tBuH_2 in C_6D_6 after purification.

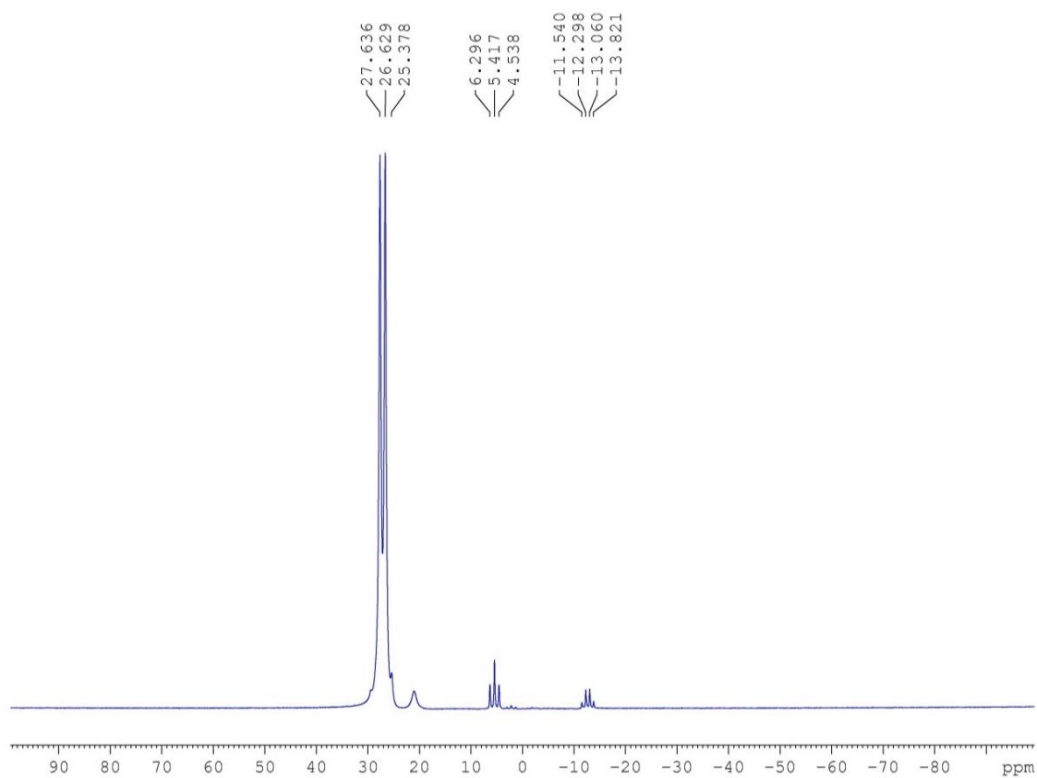


Figure S25. ^{11}B NMR of the reaction of $\text{NMe}_2\text{H}\cdot\text{BH}_3$ and N^tBuH_2 in C_6D_6 after purification.

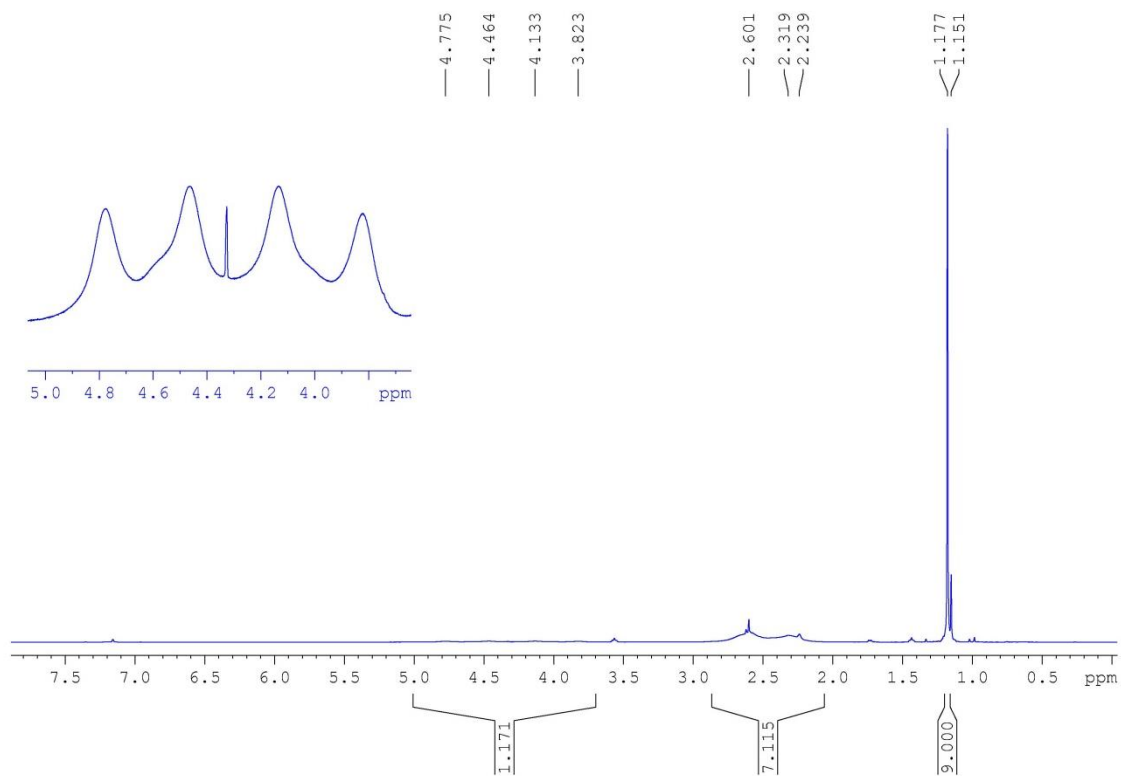


Figure S26. ^1H NMR of $(\text{N}^t\text{BuH})(\text{NMe}_2)\text{BH}$ in C_6D_6 .

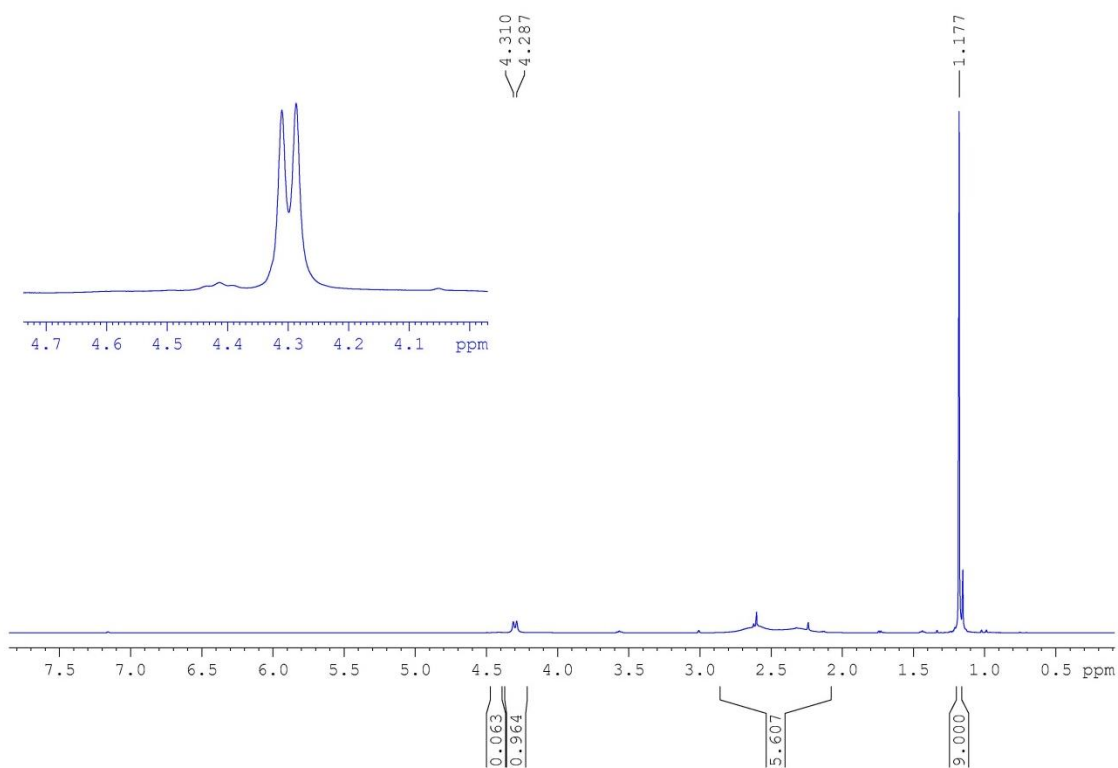


Figure S27. $^1\text{H}\{^{11}\text{B}\}$ NMR of $(\text{N}^t\text{BuH})(\text{NMe}_2)\text{BH}$ in C_6D_6 .

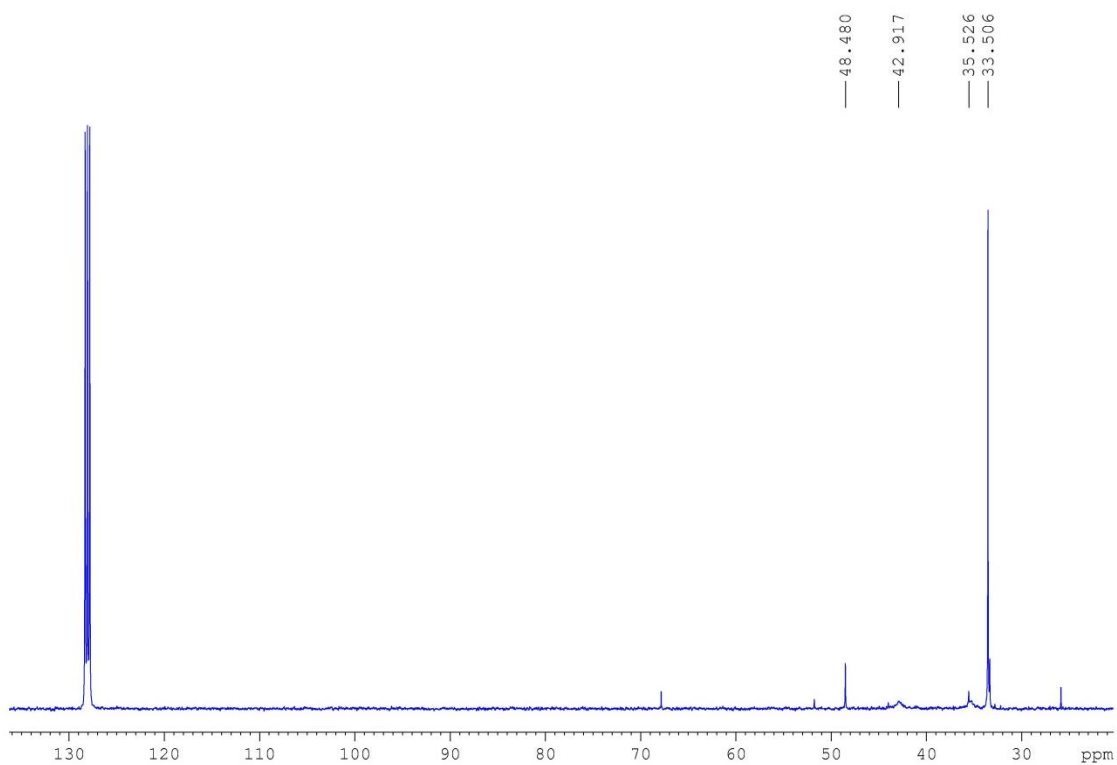


Figure S28. $^{13}\text{C}\{^1\text{H}\}$ NMR of $(\text{N}^t\text{BuH})(\text{NMe}_2)\text{BH}$ in C_6D_6 .

3.6 Diaminoborane $(\text{N}^t\text{BuH})[\text{N}(\text{CH}_2)_4]\text{BH}$.

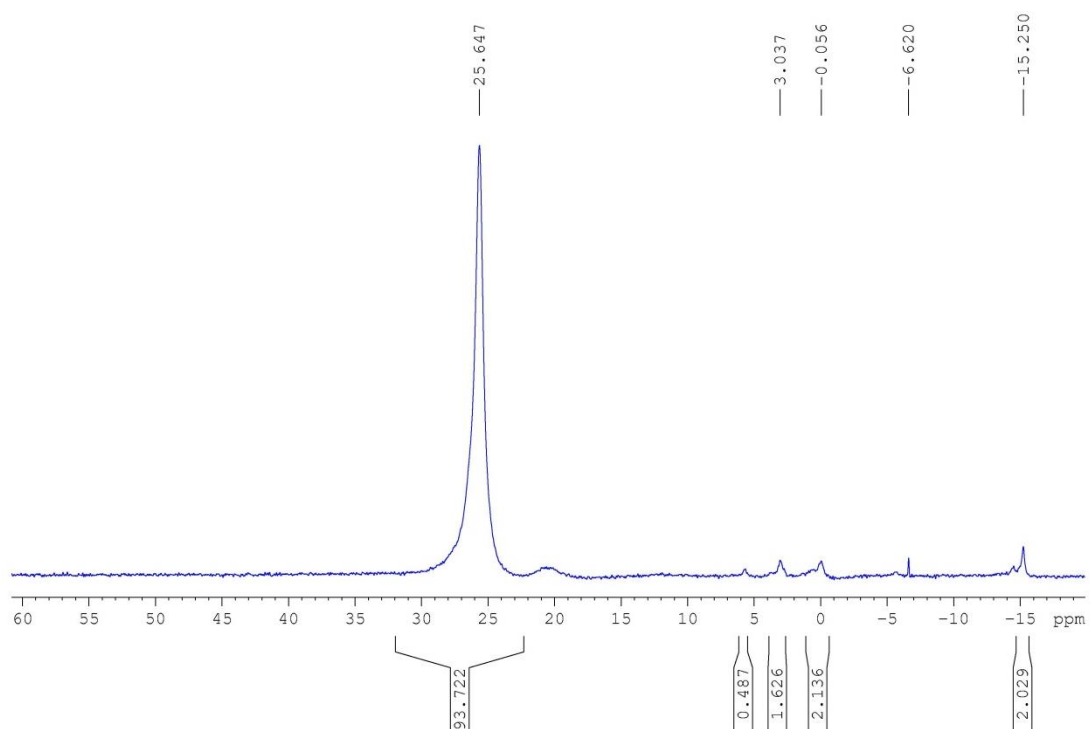


Figure S29. $^{11}\text{B}\{^1\text{H}\}$ NMR of the crude reaction mixture of $\text{N}^t\text{BuH}_2 \cdot \text{BH}_3$ and $\text{N}(\text{CH}_2)_4\text{H}$ in CD_2Cl_2 .

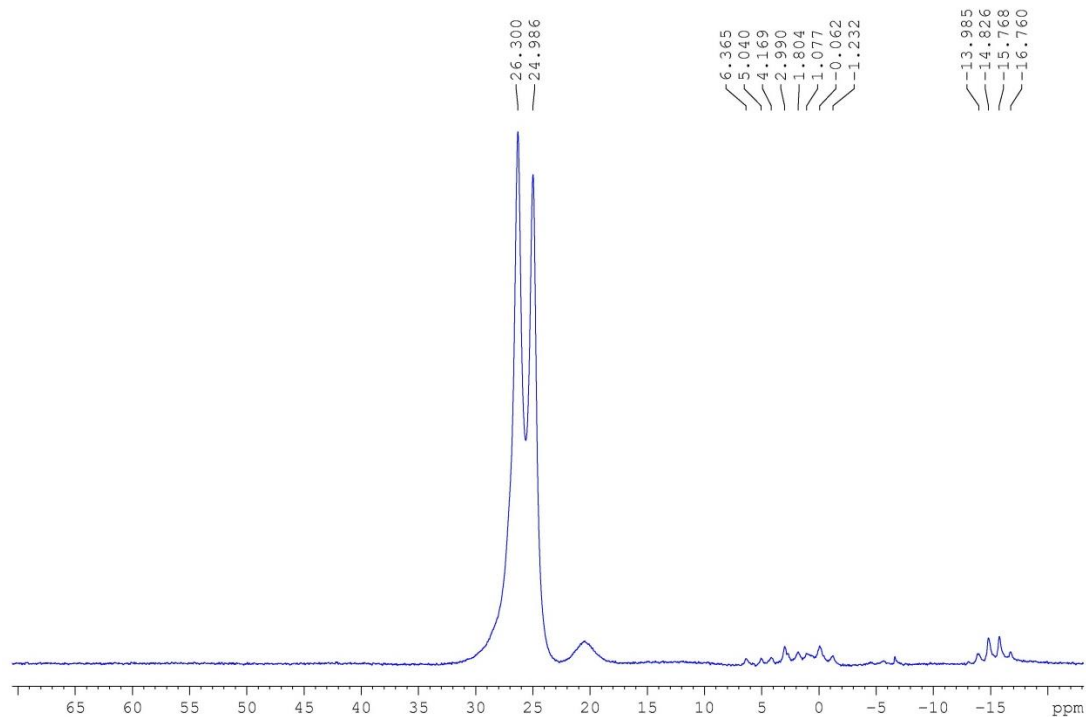


Figure S30. ^{11}B NMR of the crude reaction mixture of $\text{N}^t\text{BuH}_2\cdot\text{BH}_3$ and $\text{N}(\text{CH}_2)_4\text{H}$ in CD_2Cl_2 .

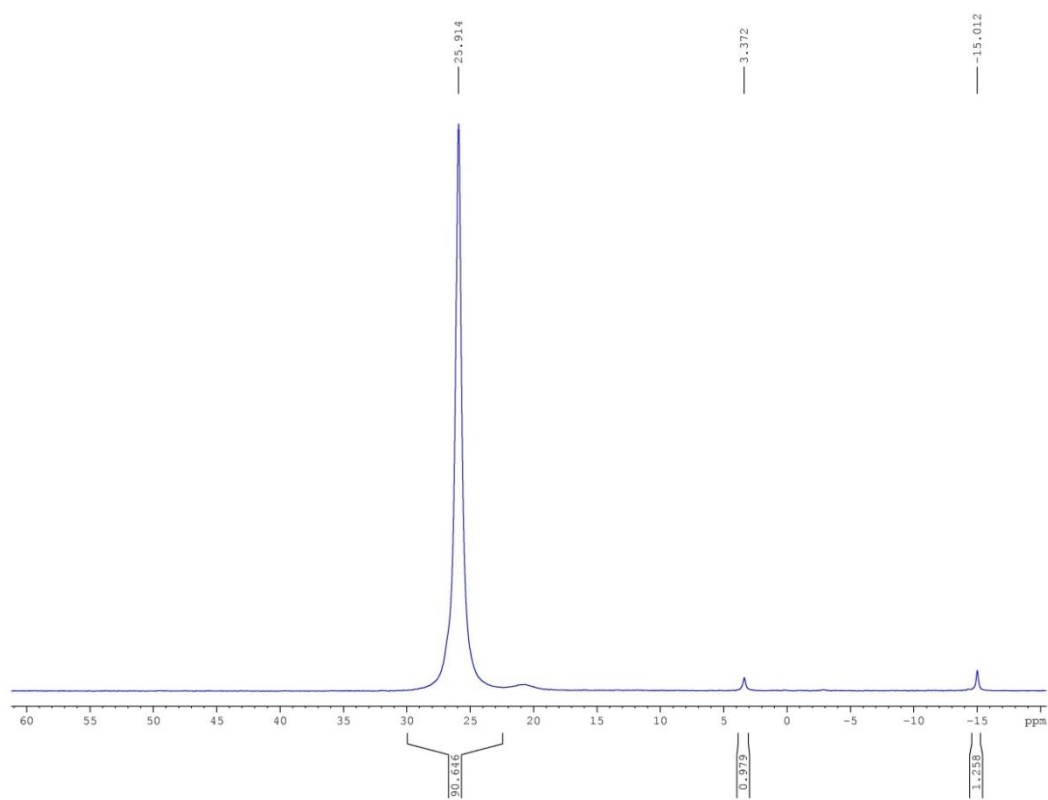


Figure S31. $^{11}\text{B}\{^1\text{H}\}$ NMR of the reaction of $\text{N}^t\text{BuH}_2\cdot\text{BH}_3$ and $\text{N}(\text{CH}_2)_4\text{H}$ in C_6D_6 after purification.

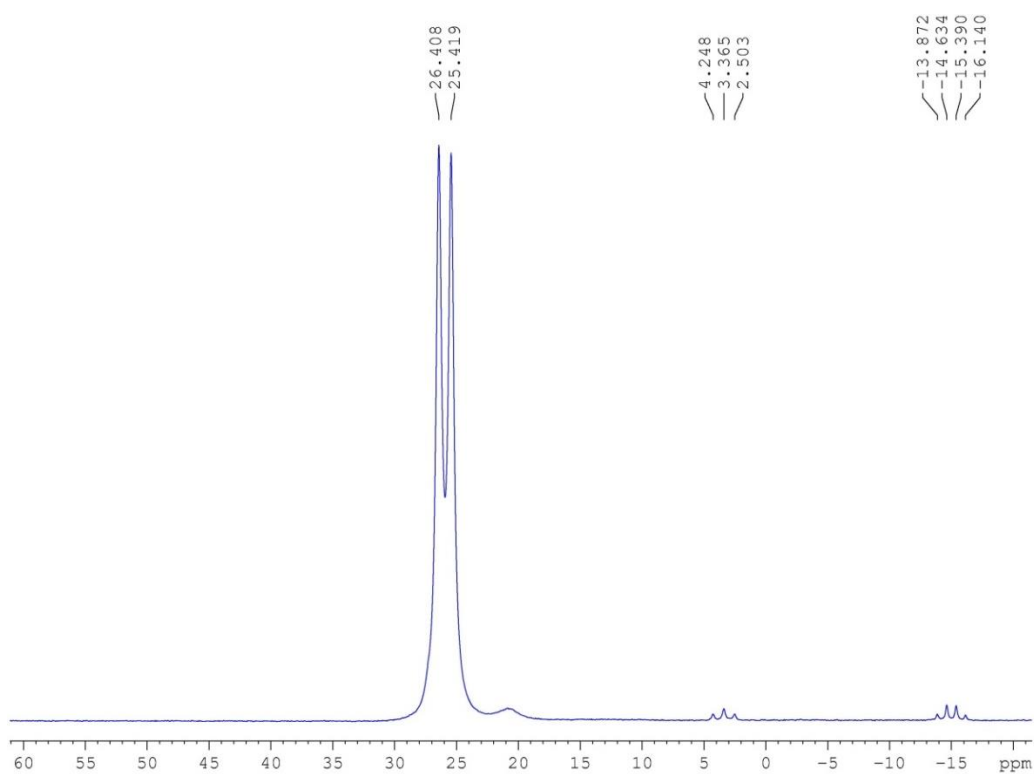


Figure S32. ^{11}B NMR of the reaction of $\text{N}^t\text{BuH}_2\cdot\text{BH}_3$ and $\text{N}(\text{CH}_2)_4\text{H}$ in C_6D_6 after purification.

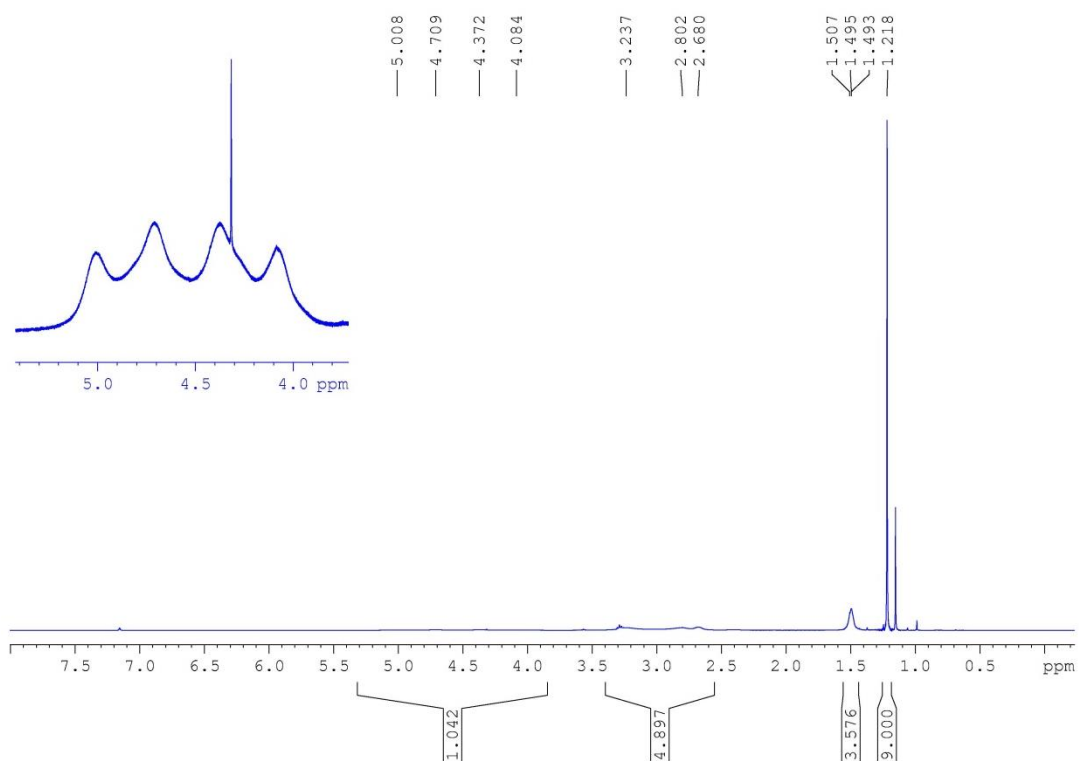


Figure S33. ^1H NMR of $(\text{N}^t\text{BuH})[\text{N}(\text{CH}_2)_4]\text{BH}$ in C_6D_6 .

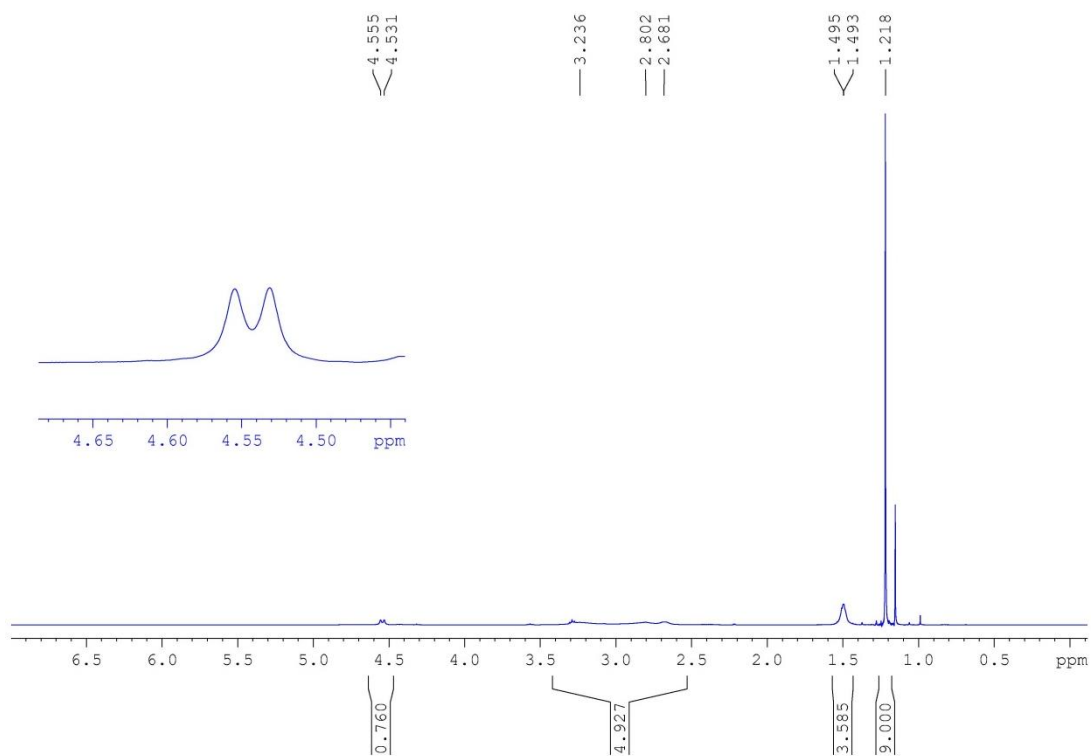


Figure S34. $^1\text{H}\{^{11}\text{B}\}$ NMR of $(\text{N}^t\text{BuH})[\text{N}(\text{CH}_2)_4]\text{BH}$ in C_6D_6 .

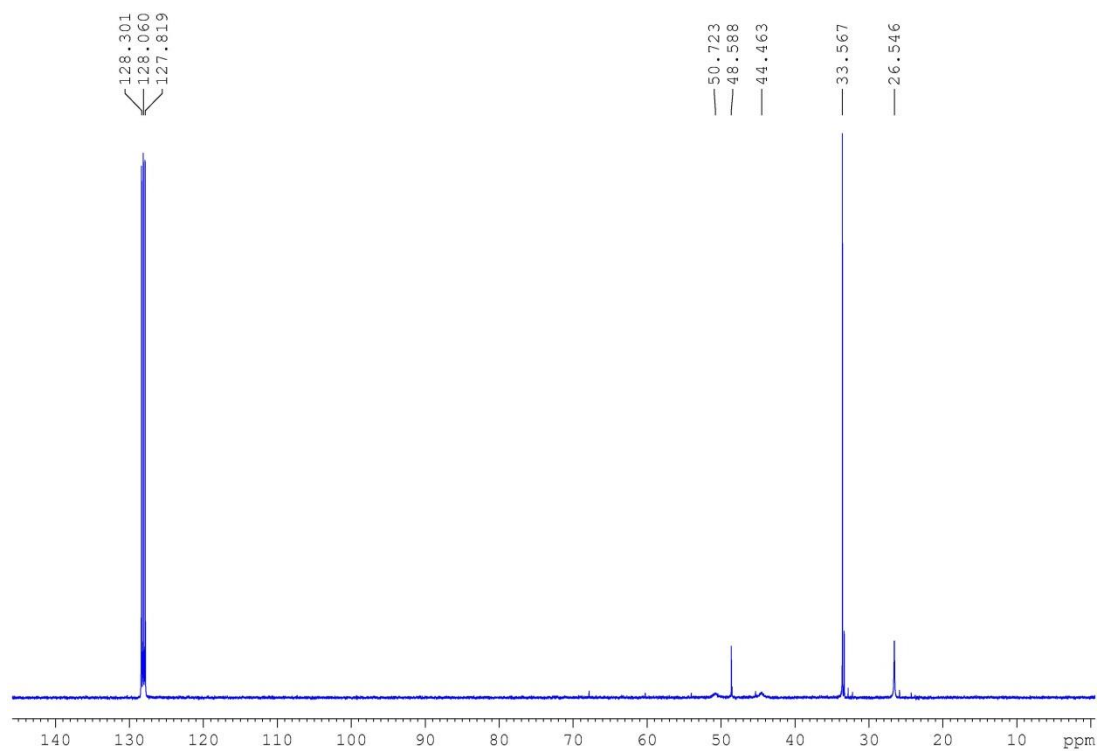


Figure S35. $^{13}\text{C}\{^1\text{H}\}$ NMR of $(\text{N}^t\text{BuH})[\text{N}(\text{CH}_2)_4]\text{BH}$ in C_6D_6 .

3.7 NMR spectra of the crude reaction mixture of $\text{NEt}_2\text{H}\cdot\text{BH}_3$ and $\text{N}(\text{CH}_2)_4\text{H}$.

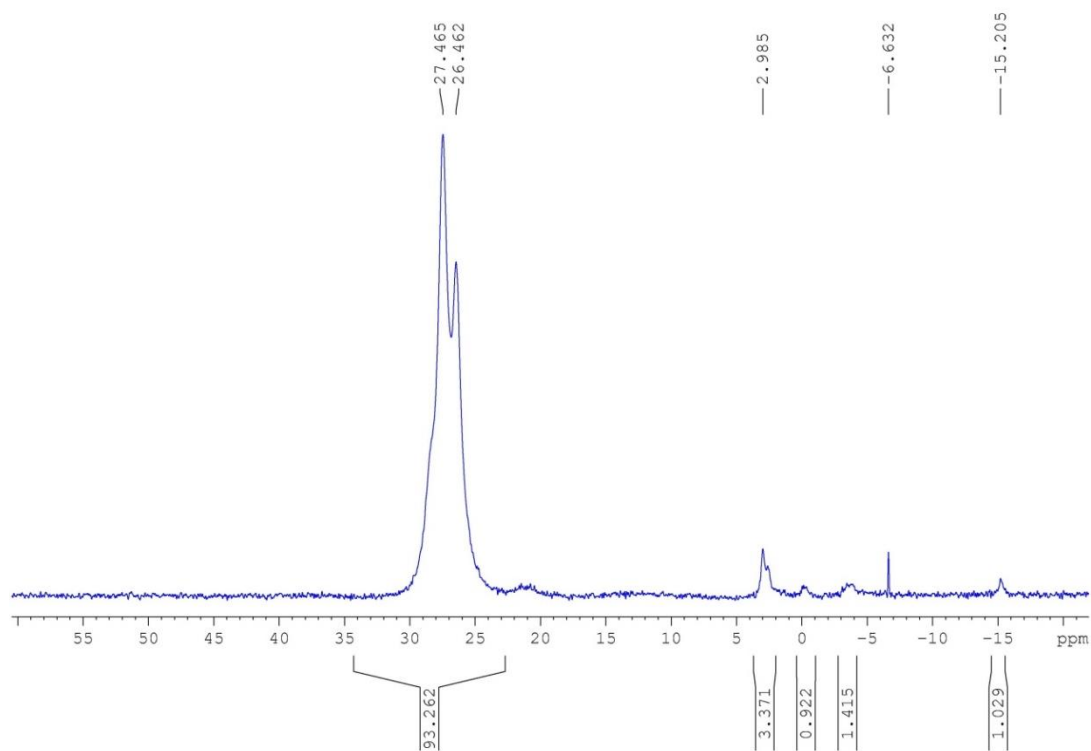


Figure S36. $^{11}\text{B}\{^1\text{H}\}$ NMR of the crude reaction mixture of $\text{NEt}_2\text{H}\cdot\text{BH}_3$ and $\text{N}(\text{CH}_2)_4\text{H}$ in CD_2Cl_2 .

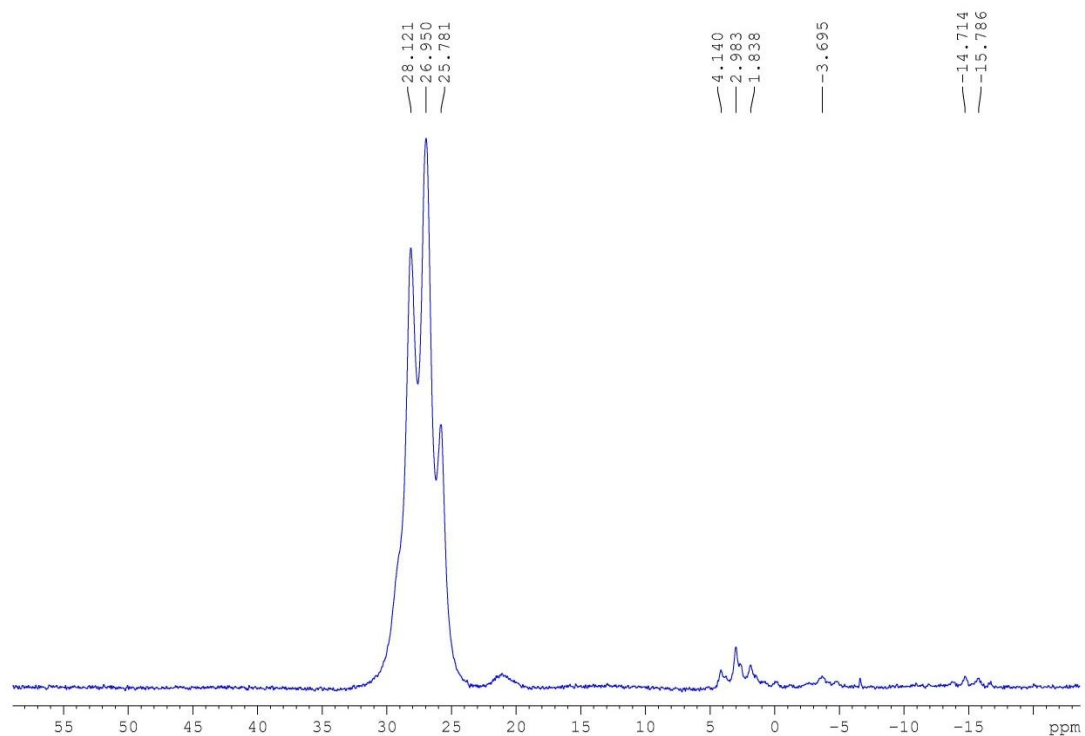


Figure S37. ^{11}B NMR of the crude reaction mixture of $\text{NEt}_2\text{H}\cdot\text{BH}_3$ and $\text{N}(\text{CH}_2)_4\text{H}$ in CD_2Cl_2 .

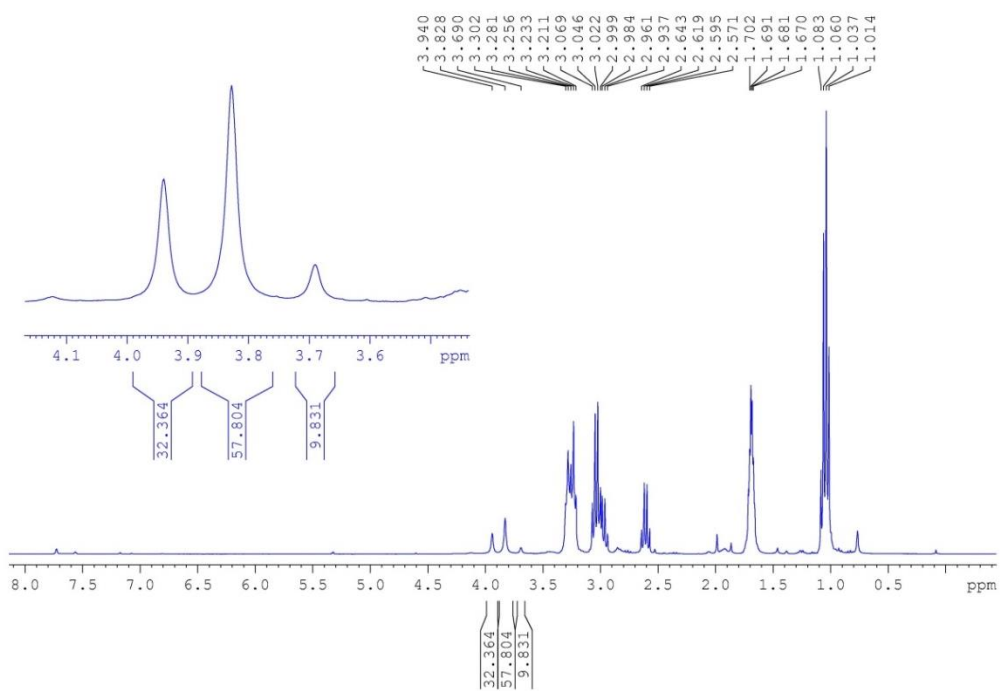


Figure S38. $^1\text{H}\{^{11}\text{B}\}$ NMR of the crude reaction mixture of $\text{NEt}_2\text{H}\cdot\text{BH}_3$ and $\text{N}(\text{CH}_2)_4\text{H}$ in CD_2Cl_2 .

3.8 NMR spectra of the crude reaction mixture of $\text{NMe}_2\text{H}\cdot\text{BH}_3$ and NEt_2H .

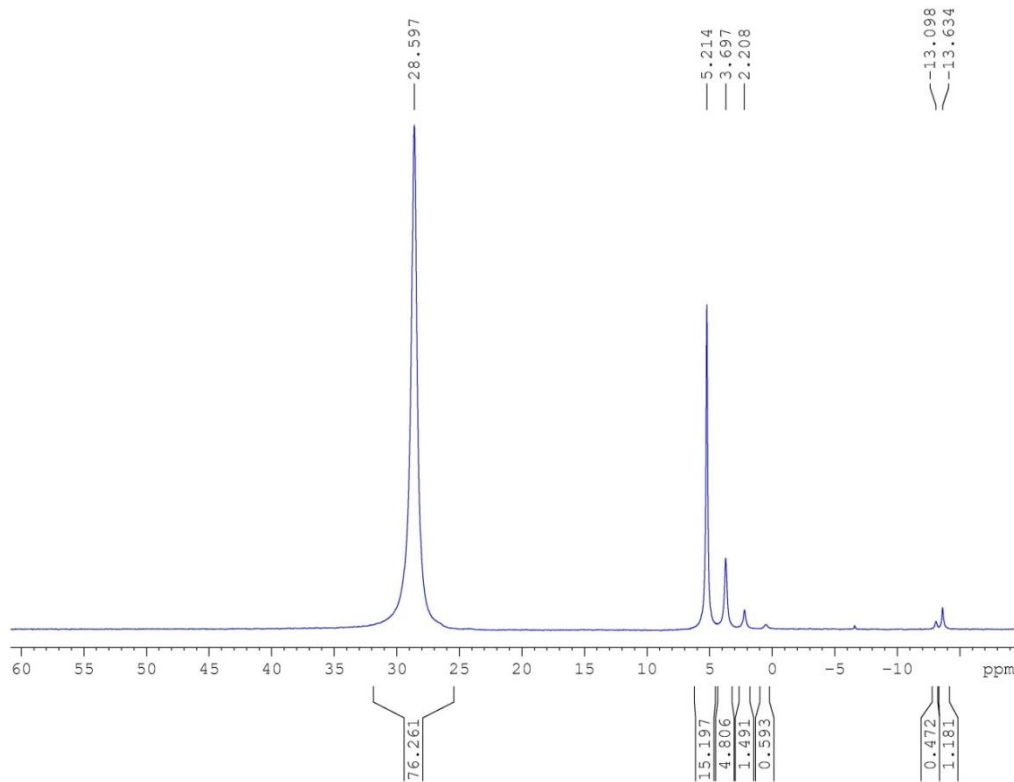


Figure S39. $^{11}\text{B}\{^1\text{H}\}$ NMR of the crude reaction mixture of $\text{NMe}_2\text{H}\cdot\text{BH}_3$ and NEt_2H in CD_2Cl_2 .

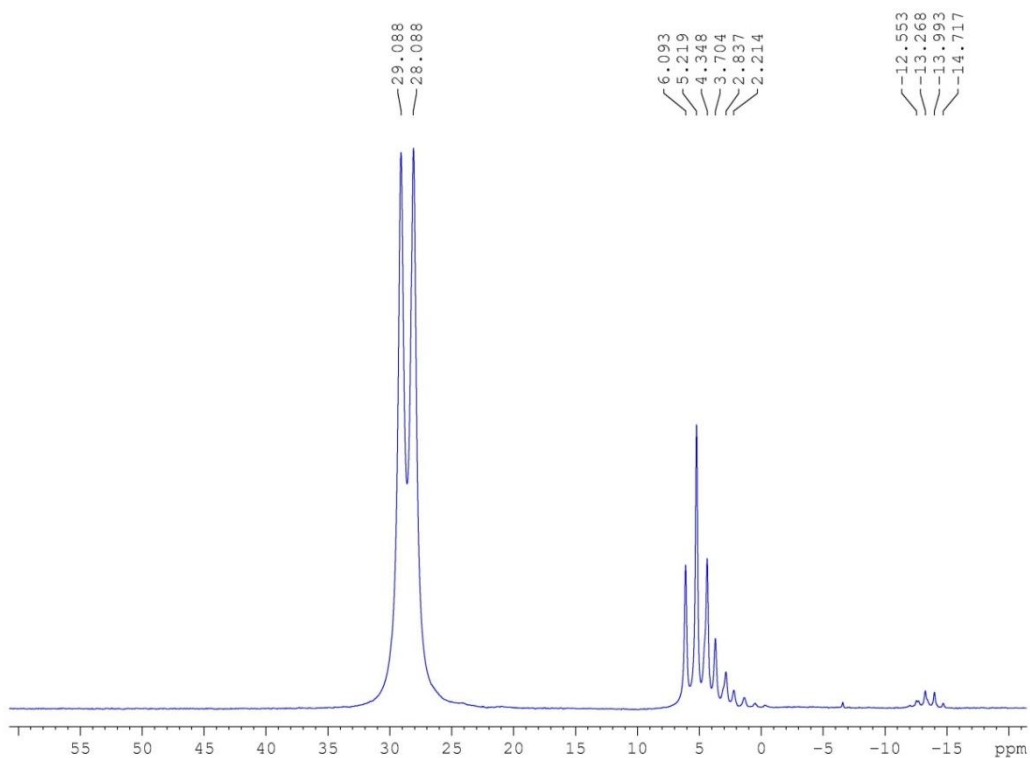


Figure S40. ^{11}B NMR of the crude reaction mixture of $\text{NMe}_2\text{H}\cdot\text{BH}_3$ and NEt_2H in CD_2Cl_2 .

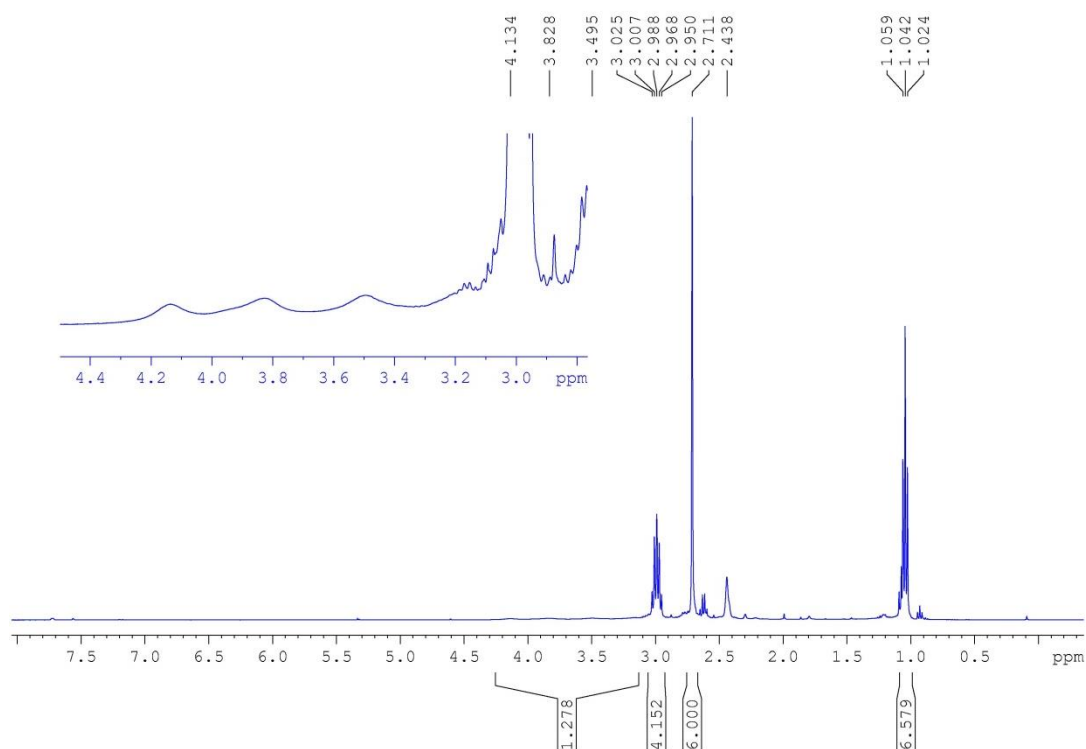


Figure S41. ^1H NMR of the crude reaction mixture of $\text{NMe}_2\text{H}\cdot\text{BH}_3$ and NEt_2H in CD_2Cl_2 .

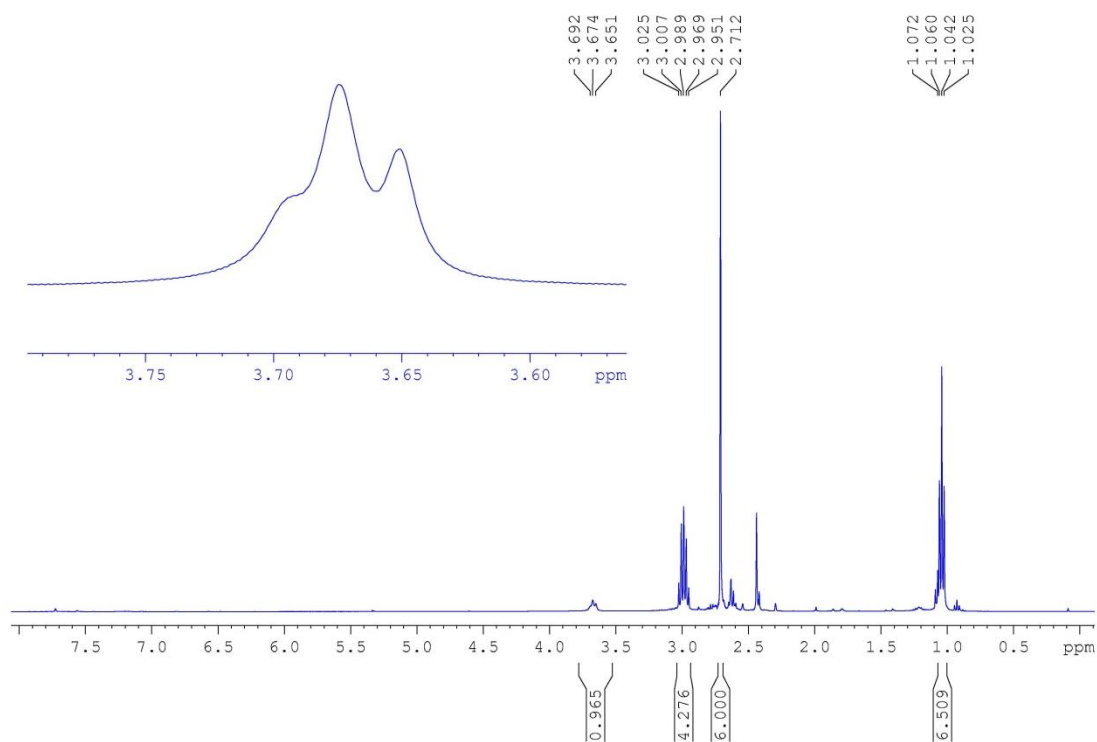


Figure S42. $^1\text{H}\{^{11}\text{B}\}$ NMR of the crude reaction mixture of $\text{NMe}_2\text{H}\cdot\text{BH}_3$ and NEt_2H in CD_2Cl_2 .

4. NMR SPECTRA OF COMPLEX 3c.

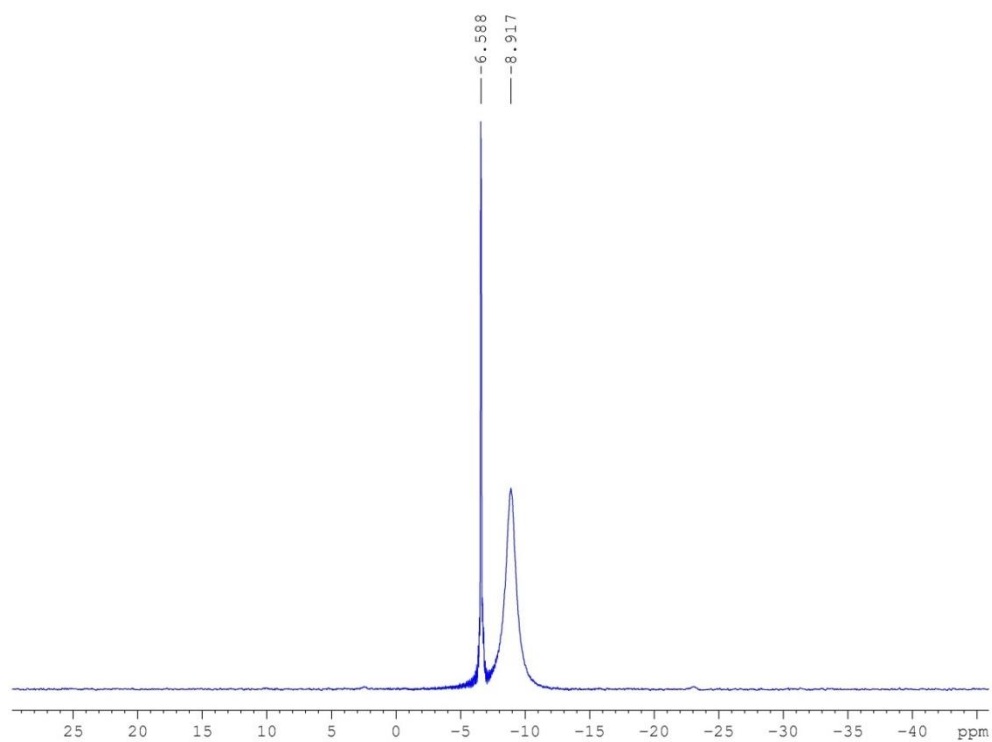


Figure S43. $^{11}\text{B}\{^1\text{H}\}$ NMR of complex $[\text{Pt}(\text{I}'\text{Bu}')(\text{I}'\text{Bu})(\text{H}_3\text{B}\cdot\text{Py})][\text{BAr}^{\text{F}}]$ (**3c**) in CD_2Cl_2 at 298 K.

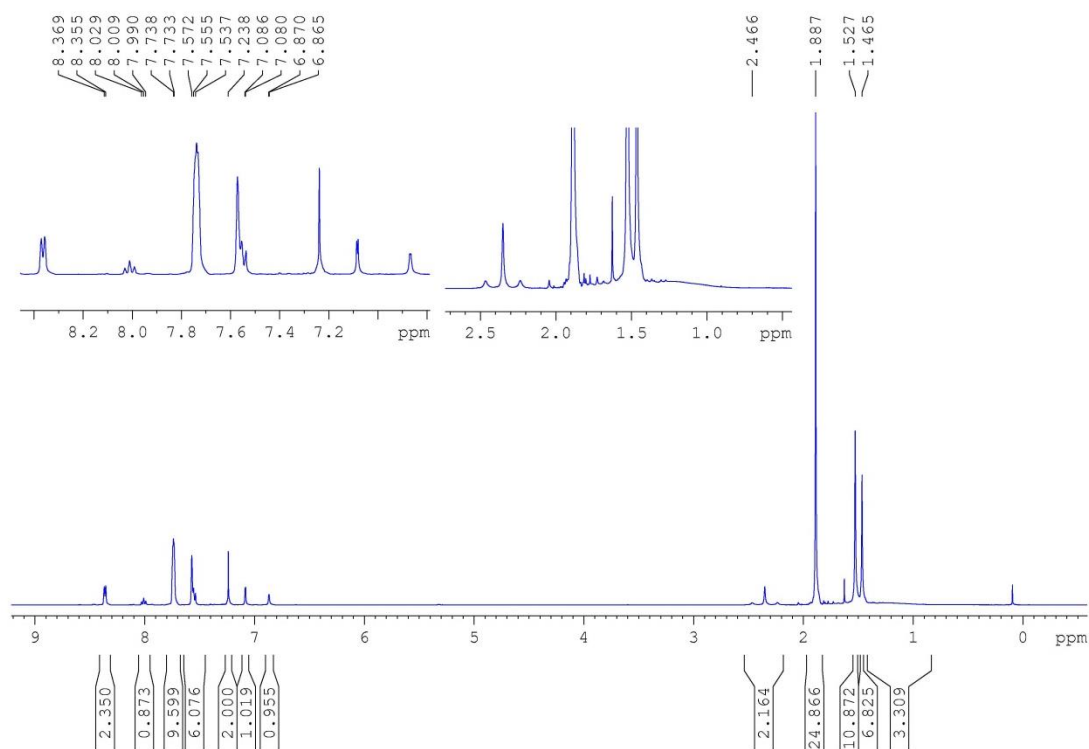


Figure S44. ^1H NMR of complex $[\text{Pt}(\text{I}^t\text{Bu}')(\text{I}^i\text{Bu})(\text{H}_3\text{B}\cdot\text{C}_5\text{H}_5\text{N})][\text{BAR}^{\text{F}}]$ (**3c**) in CD_2Cl_2 at 298 K.

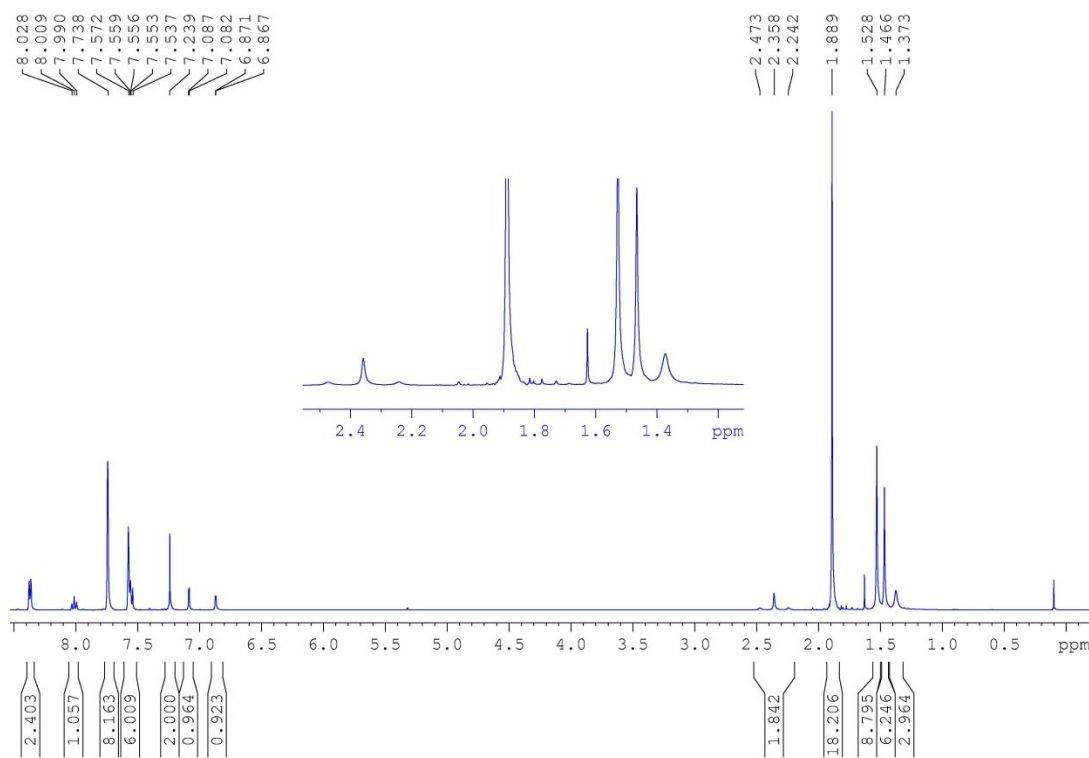


Figure S45. $^1\text{H}\{^{11}\text{B}\}$ NMR of complex $[\text{Pt}(\text{I}^t\text{Bu}')(\text{I}^i\text{Bu})(\text{H}_3\text{B}\cdot\text{C}_5\text{H}_5\text{N})][\text{BAR}^{\text{F}}]$ (**3c**) in CD_2Cl_2 at 298 K.

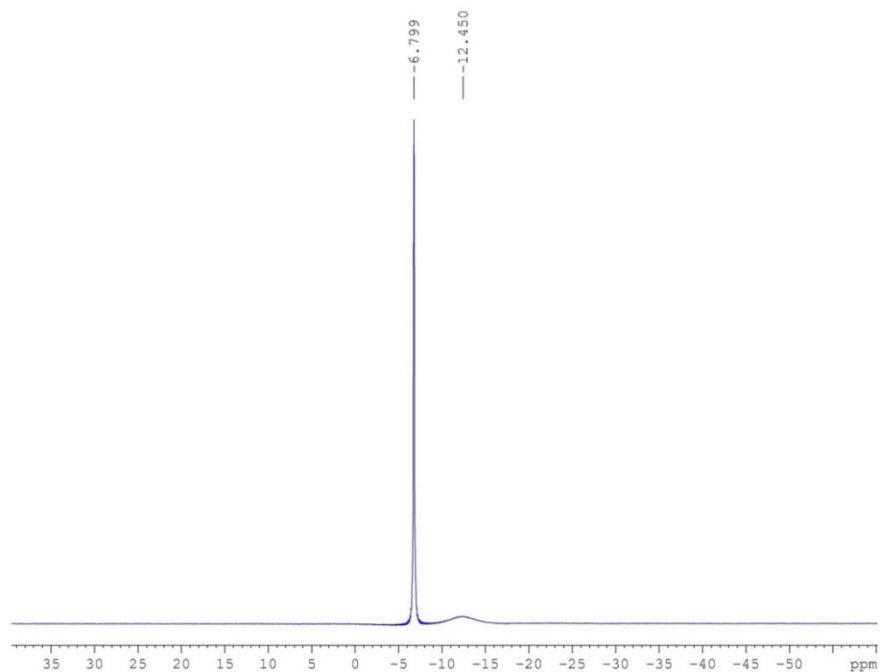


Figure S46. $^{11}\text{B}\{^1\text{H}\}$ NMR of complex $[\text{Pt}(\text{I}^t\text{Bu}')(\text{I}^t\text{Bu})(\text{H}_3\text{B}\cdot\text{C}_5\text{H}_5\text{N})][\text{BAr}^{\text{F}}]$ (**3c**) in CD_2Cl_2 at 183 K.

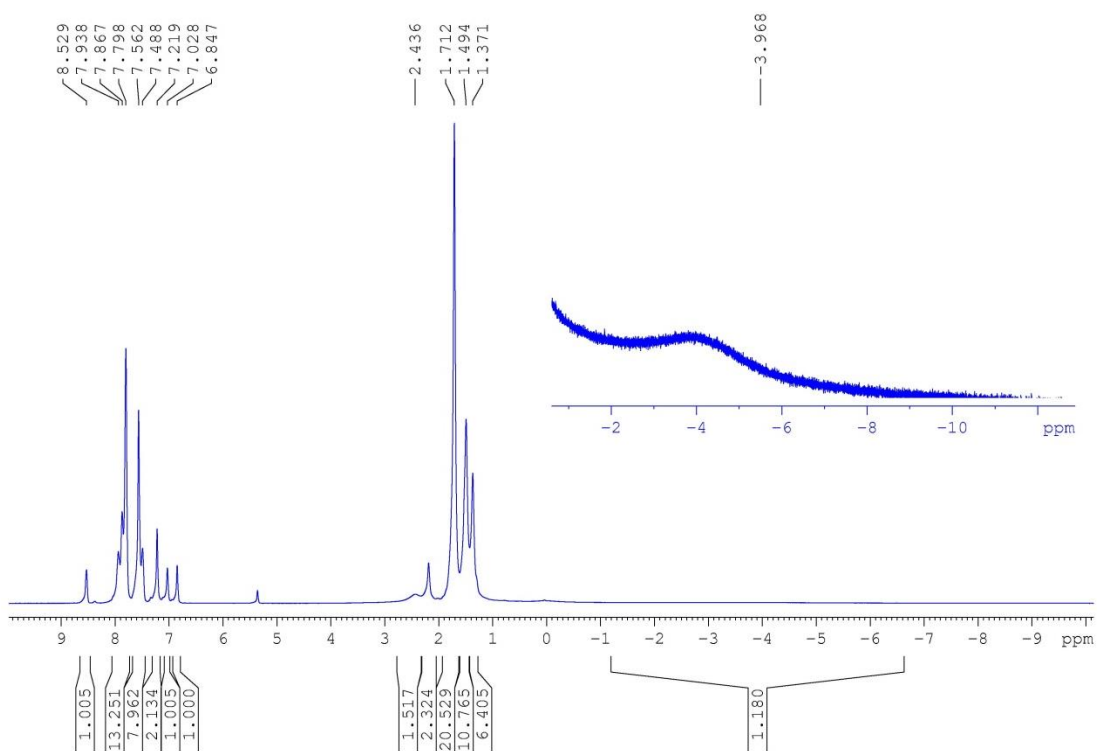


Figure S47. ^1H NMR of complex $[\text{Pt}(\text{I}^t\text{Bu}')(\text{I}^t\text{Bu})(\text{H}_3\text{B}\cdot\text{C}_5\text{H}_5\text{N})][\text{BAr}^{\text{F}}]$ (**3c**) in CD_2Cl_2 at 183 K.

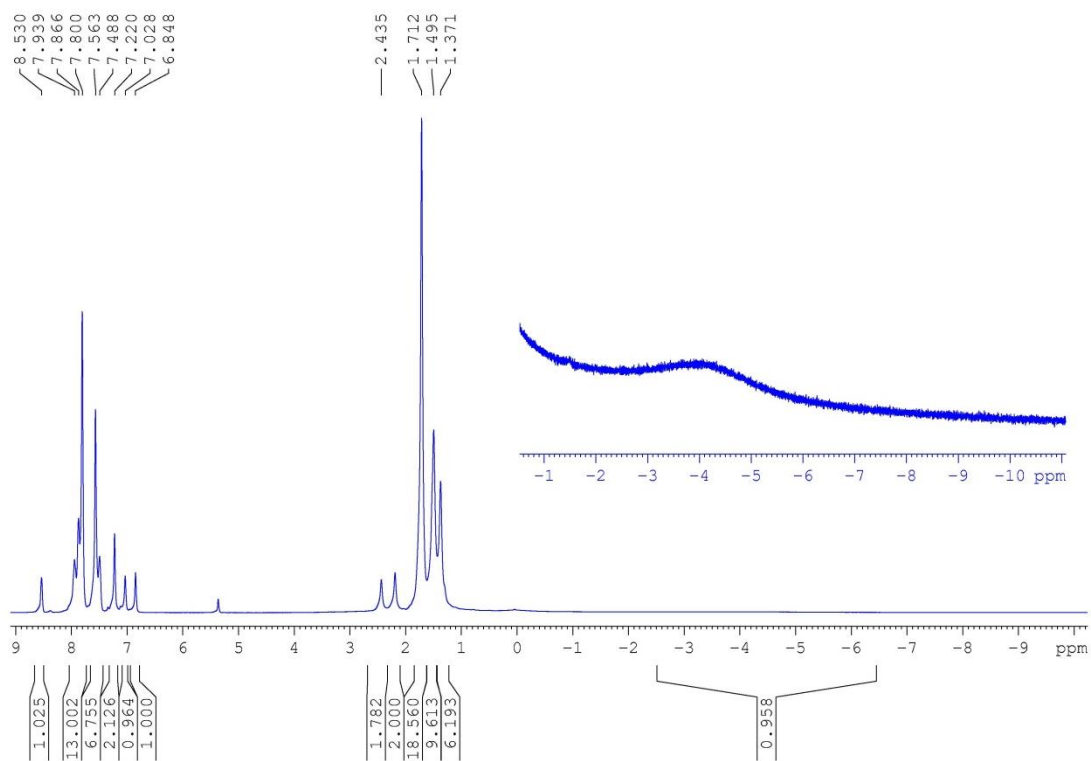


Figure S48. $^1\text{H}\{^{11}\text{B}\}$ NMR of complex $[\text{Pt}(\text{I}^t\text{Bu}')(\text{I}^t\text{Bu})(\text{H}_3\text{B}\cdot\text{C}_5\text{H}_5\text{N})][\text{BAr}^{\text{F}}]$ (**3c**) in CD_2Cl_2 at 183 K.

5. NMR SPECTRA OF A MIXTURE OF 4 AND $\text{H}_3\text{B}\cdot\text{C}_5\text{H}_5\text{N}$.

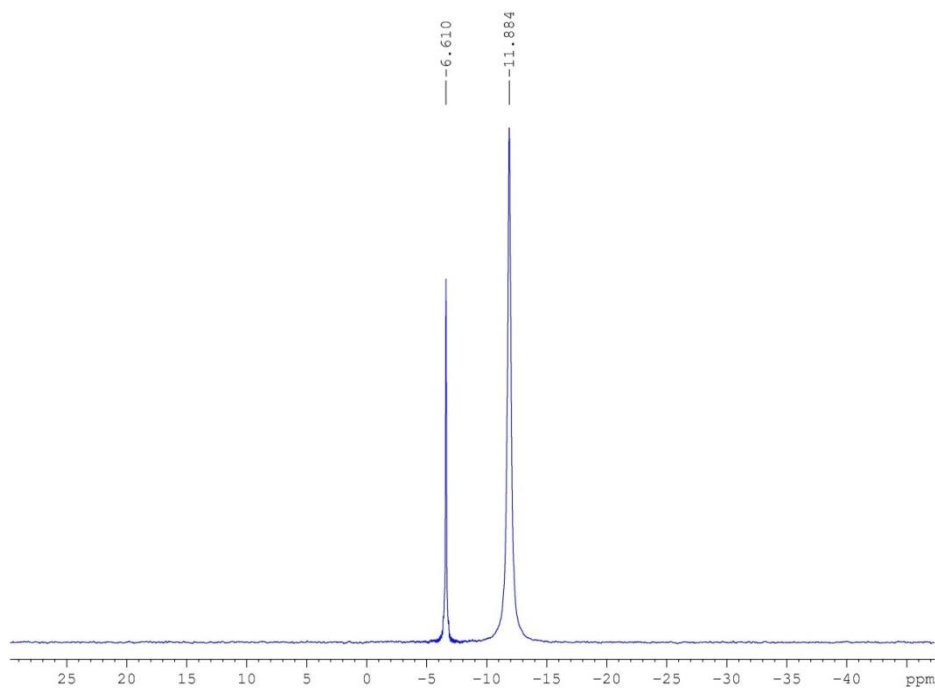


Figure S49. $^{11}\text{B}\{^1\text{H}\}$ NMR of a mixture of complex $[\text{PtH}(\text{I}^t\text{Bu})_2][\text{BAr}^{\text{F}}]$ (**4**) and $\text{H}_3\text{B}\cdot\text{C}_5\text{H}_5\text{N}$ in CD_2Cl_2 at 298 K.

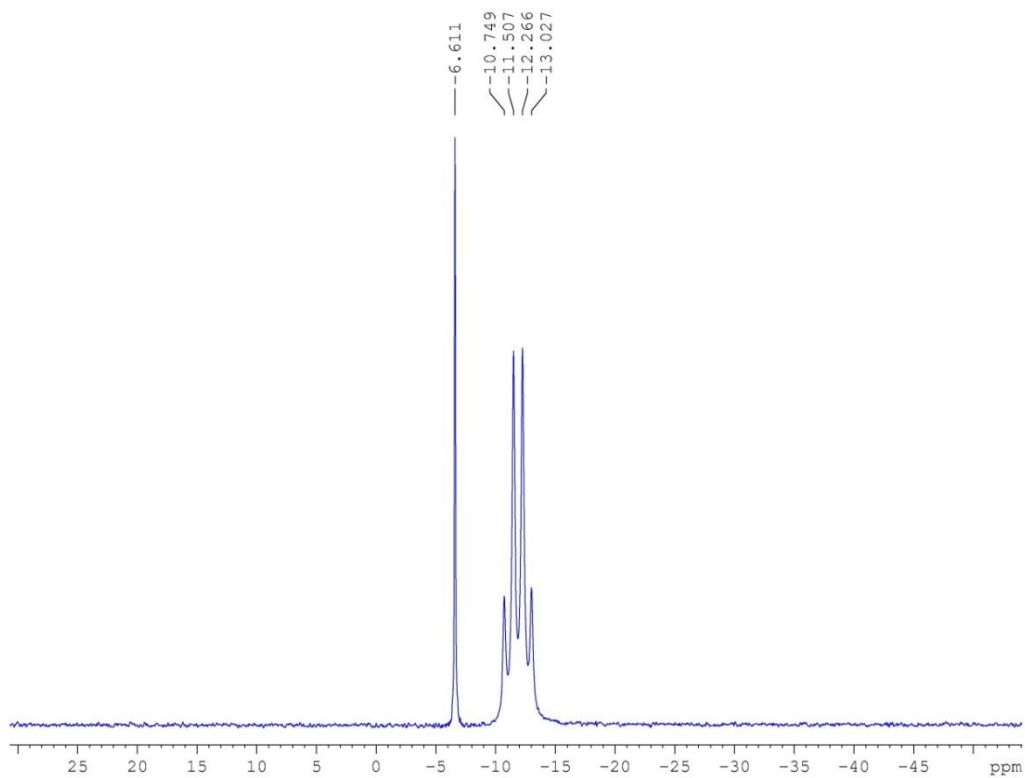


Figure S50. ^{11}B NMR of a mixture of complex $[\text{PtH}(\text{tBu})_2][\text{BAR}^{\text{F}}]$ (**4**) and $\text{H}_3\text{B}\cdot\text{C}_5\text{H}_5\text{N}$ in CD_2Cl_2 at 298 K.

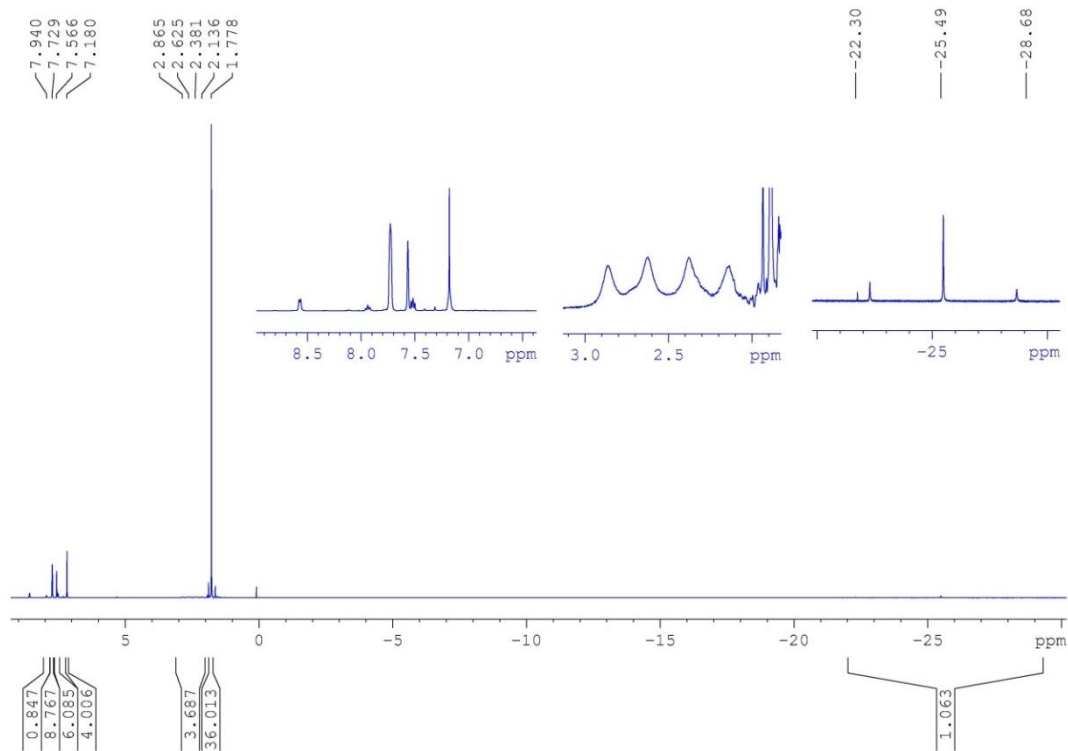


Figure S51. ^1H NMR of a mixture of complex $[\text{PtH}(\text{tBu})_2][\text{BAR}^{\text{F}}]$ (**4**) and $\text{H}_3\text{B}\cdot\text{C}_5\text{H}_5\text{N}$ in CD_2Cl_2 at 298 K.

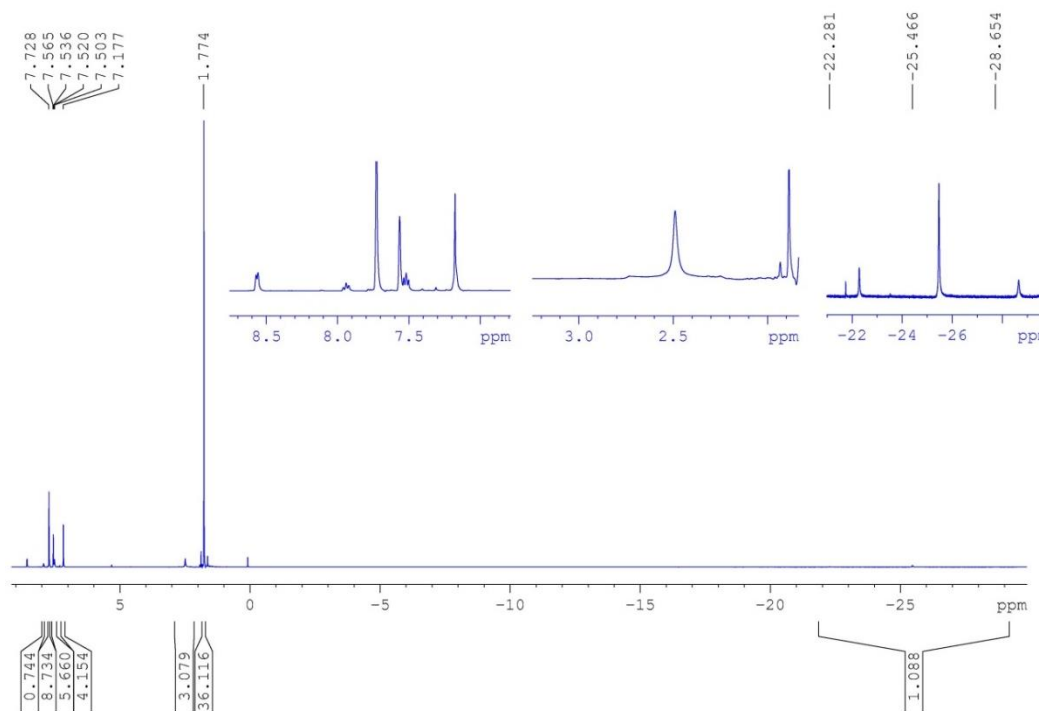


Figure S52. $^1\text{H}\{^{11}\text{B}\}$ NMR of a mixture of complex $[\text{PtH}(\text{I}'\text{Bu})_2][\text{BAR}^{\text{F}}]$ (**4**) and $\text{H}_3\text{B}\cdot\text{C}_5\text{H}_5\text{N}$ in CD_2Cl_2 at 298 K.

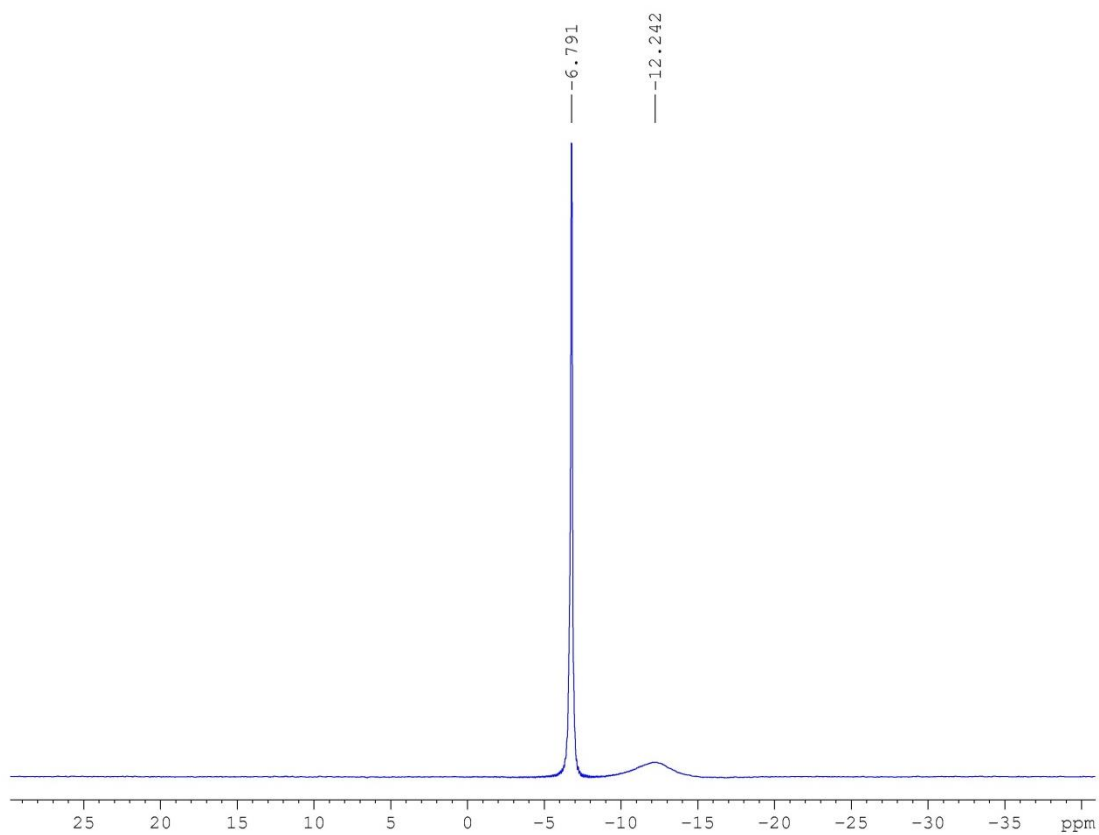


Figure S53. $^{11}\text{B}\{^1\text{H}\}$ NMR of a mixture of complex $[\text{PtH}(\text{I}'\text{Bu})_2][\text{BAR}^{\text{F}}]$ (**4**) and $\text{H}_3\text{B}\cdot\text{C}_5\text{H}_5\text{N}$ in CD_2Cl_2 at 188 K.

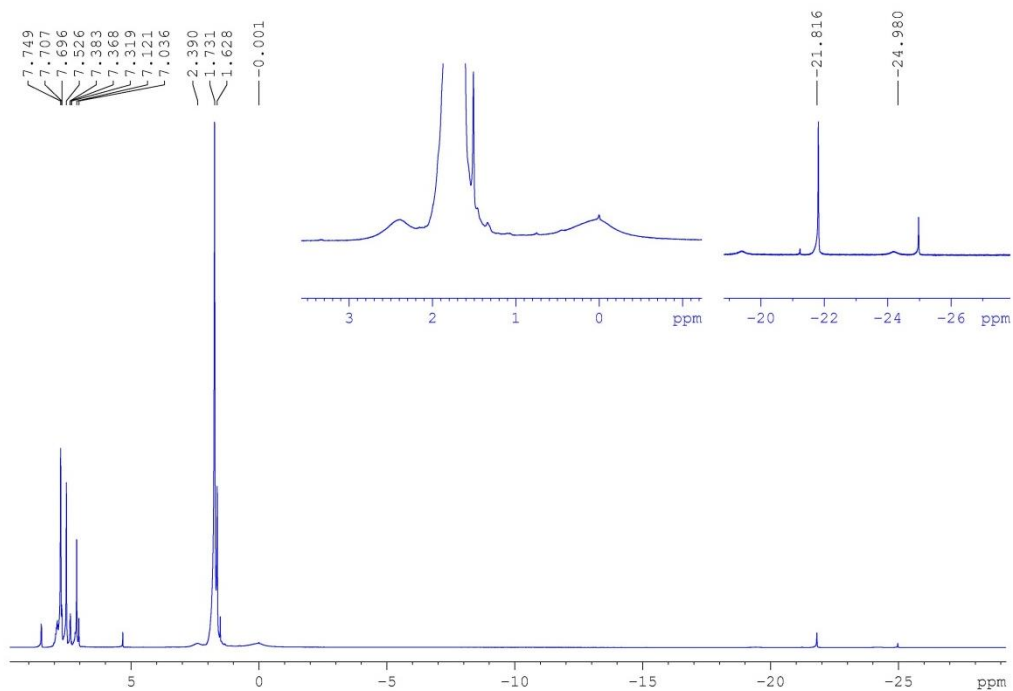


Figure S54. ^1H NMR of a mixture of complex $[\text{PtH}(\text{I}'\text{Bu})_2][\text{BAR}^{\text{F}}]$ (**4**) and $\text{H}_3\text{B}\cdot\text{C}_5\text{H}_5\text{N}$ in CD_2Cl_2 at 188 K.

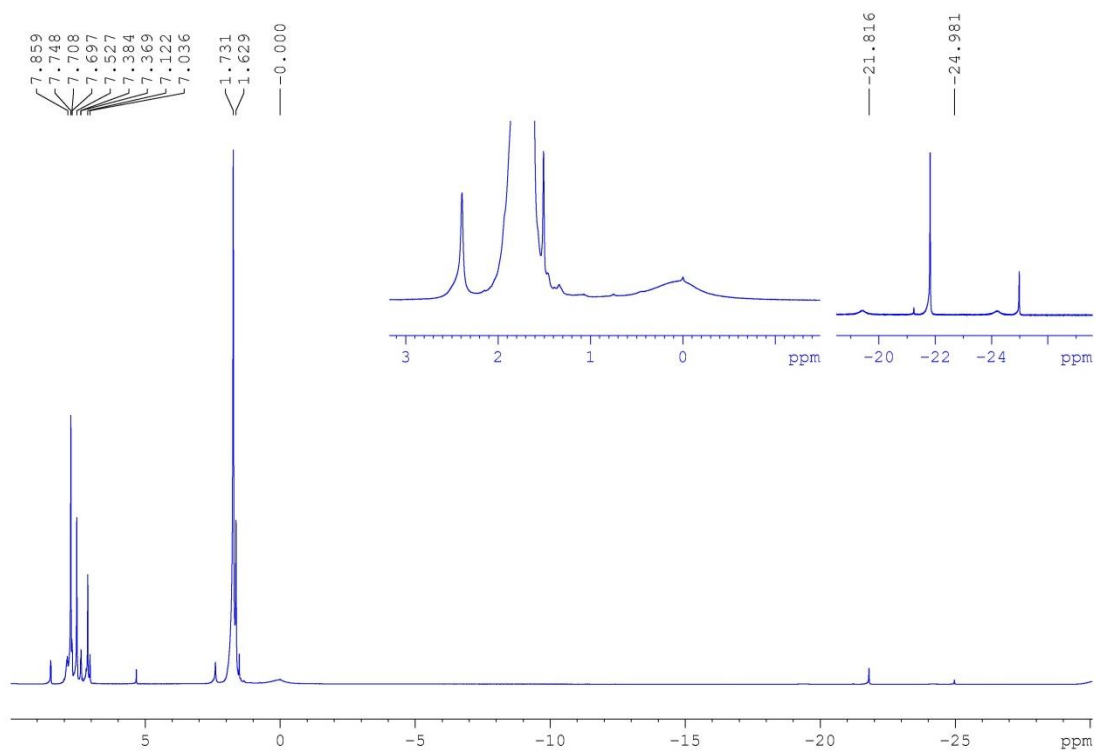


Figure S55. $^1\text{H}\{^{11}\text{B}\}$ NMR of a mixture of complex $[\text{PtH}(\text{I}'\text{Bu})_2][\text{BAR}^{\text{F}}]$ (**4**) and $\text{H}_3\text{B}\cdot\text{C}_5\text{H}_5\text{N}$ in CD_2Cl_2 at 188 K.

6. H₂ EVOLUTION GRAPHICS IN A CLOSED REACTION VESSEL.

In some of the kinetic profiles (see below) an increase in the reaction rate was observed at the end of the process (see for example Figure S56). In order to check if this effect was due to an autocatalytic process, the reaction of ^tBuNH₂·BH₃ and ^tBuNH₂ was carried out in the presence of 100% of (^tBuNH)₂BH. Nevertheless, no dehydrocoupling was observed under these reaction conditions, whereas injection of 0.5% of catalyst **1** into this reaction media resulted in an immediately H₂ release with an identical kinetic profile than that observed in the absence of (^tBuNH)₂BH.

Additionally, since sigmoid-like kinetic shapes are usually associated to the formation of nanoparticles, a poisoning experiment using a large excess of Hg (1000 equiv) was performed. Nevertheless, the reaction proceeded at almost the same rate with identical kinetic profile, clearly indicating that no nanoparticles or colloids were formed during catalysis (see Fig. S57).

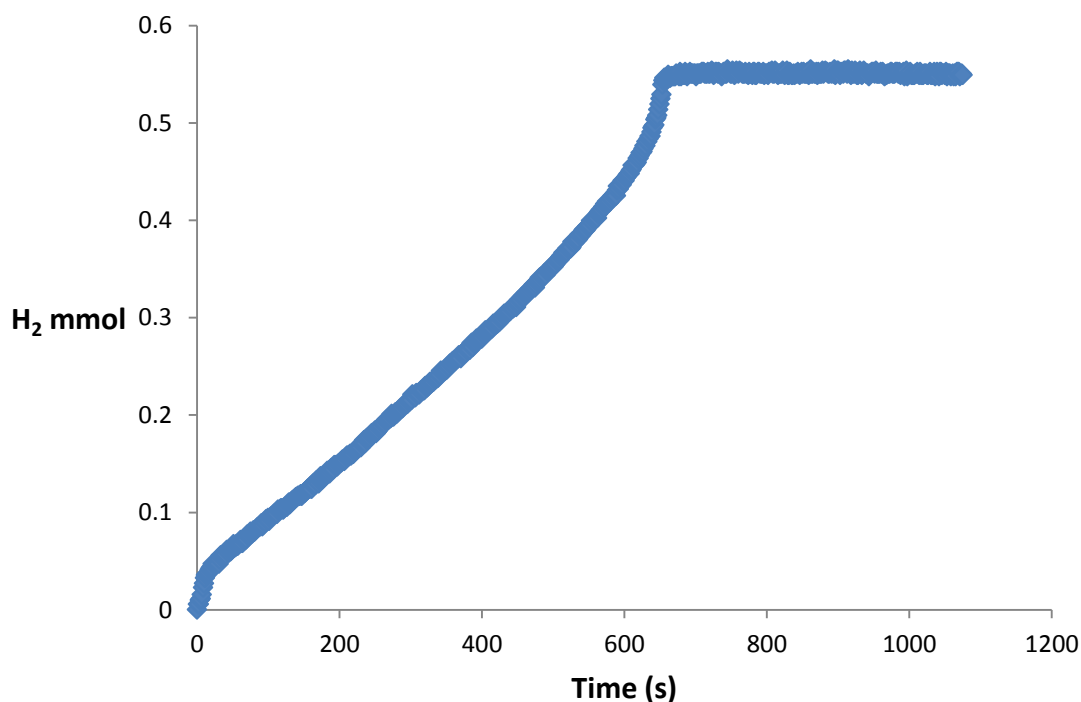


Figure S56. Monitoring the amount of H₂ released in the catalytic dehydrocoupling of N^tBuH₂·BH₃ and N^tBuH₂ with 0.5 % of complex **1**.

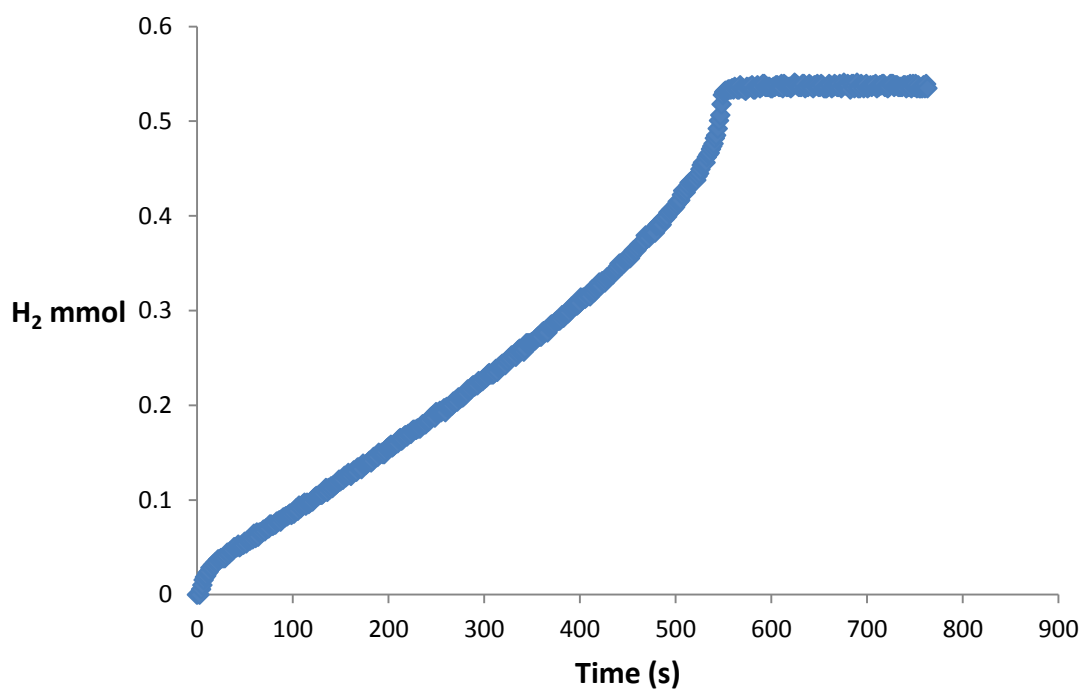


Figure S57. Monitoring the amount of H₂ released in the catalytic dehydrocoupling of N^tBuH₂·BH₃ and N^tBuH₂ with 0.5 % of complex **1** in the presence of 1000 eq of Hg.

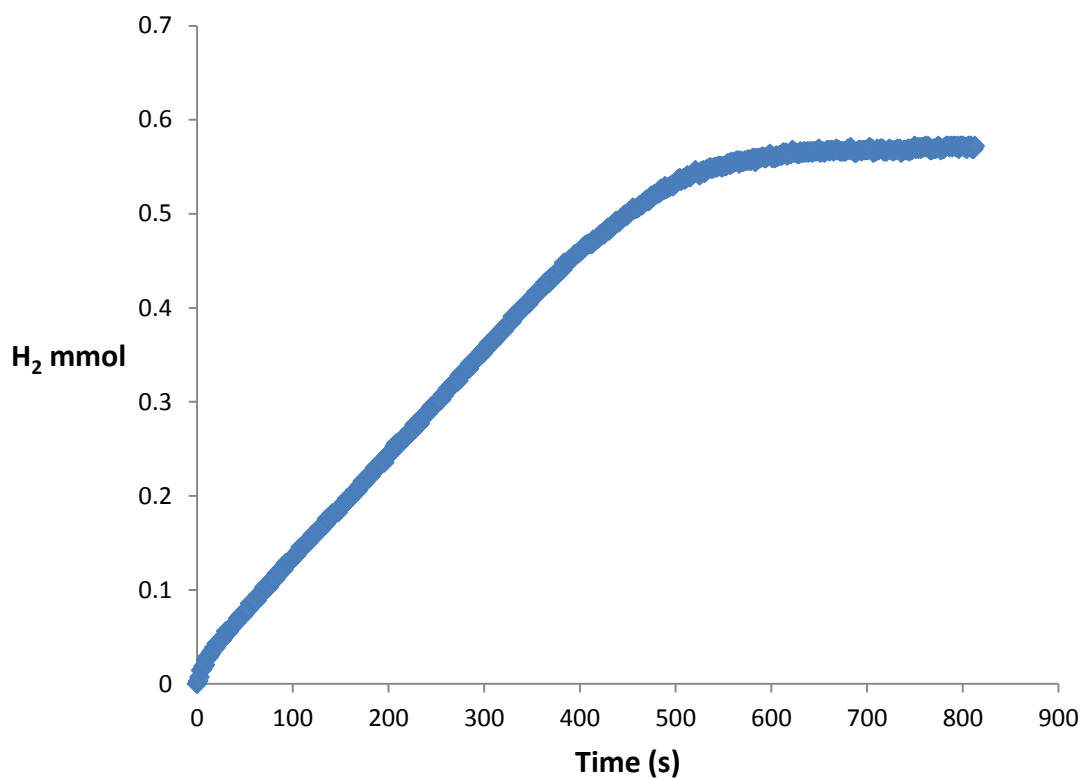


Figure S58. Monitoring the amount of H₂ released in the catalytic dehydrocoupling of NEt₂H·BH₃ and NEt₂H with 0.5 % of complex **1**.

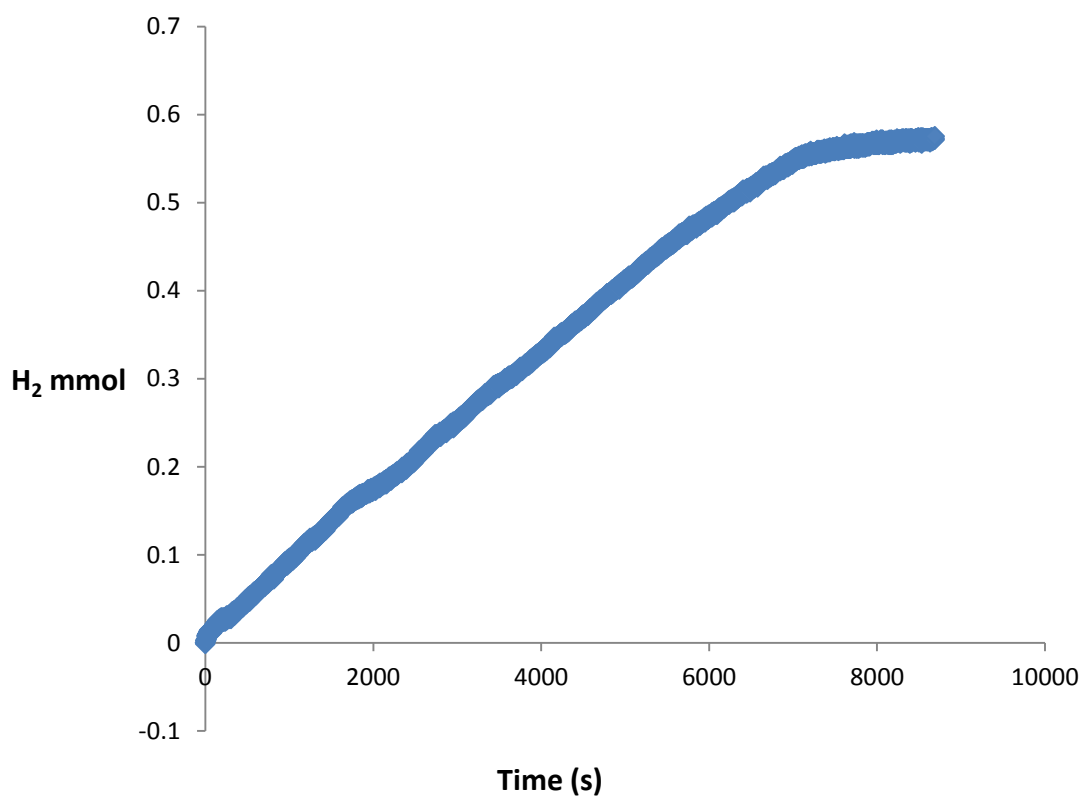


Figure S59. Monitoring the amount of H₂ released in the catalytic dehydrocoupling of N(CH₂)₄H·BH₃ and N(CH₂)₄H with 0.5 % of complex **1**.

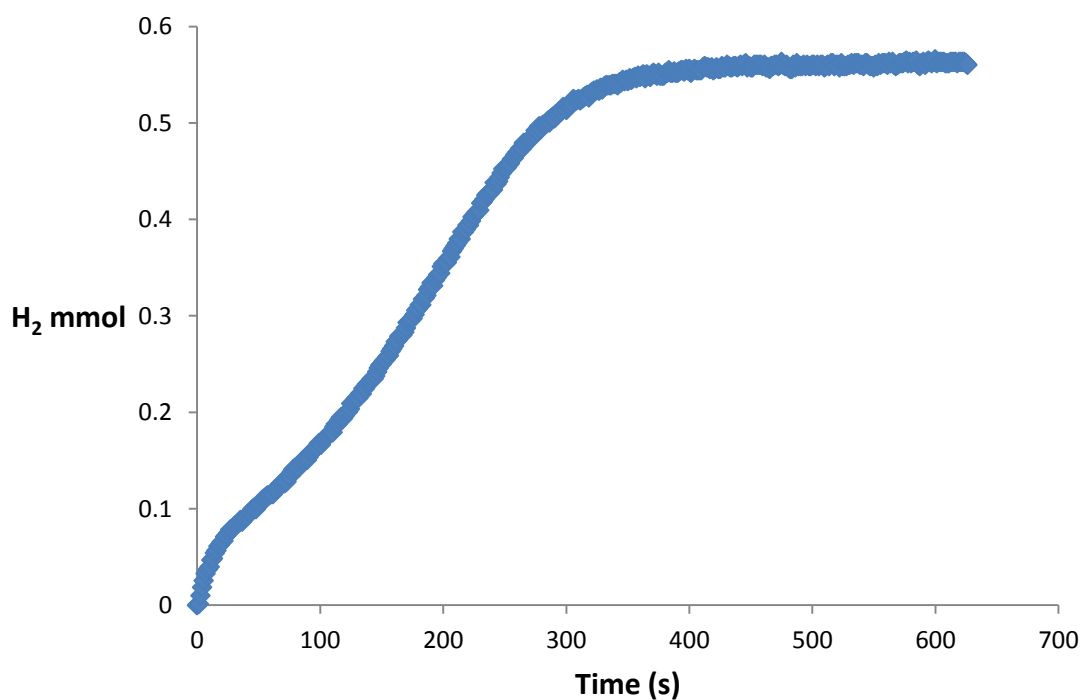


Figure S60. Monitoring the amount of H₂ released in the catalytic dehydrocoupling of N^tBuH₂·BH₃ and NEt₂H with 0.5 % of complex **1**.

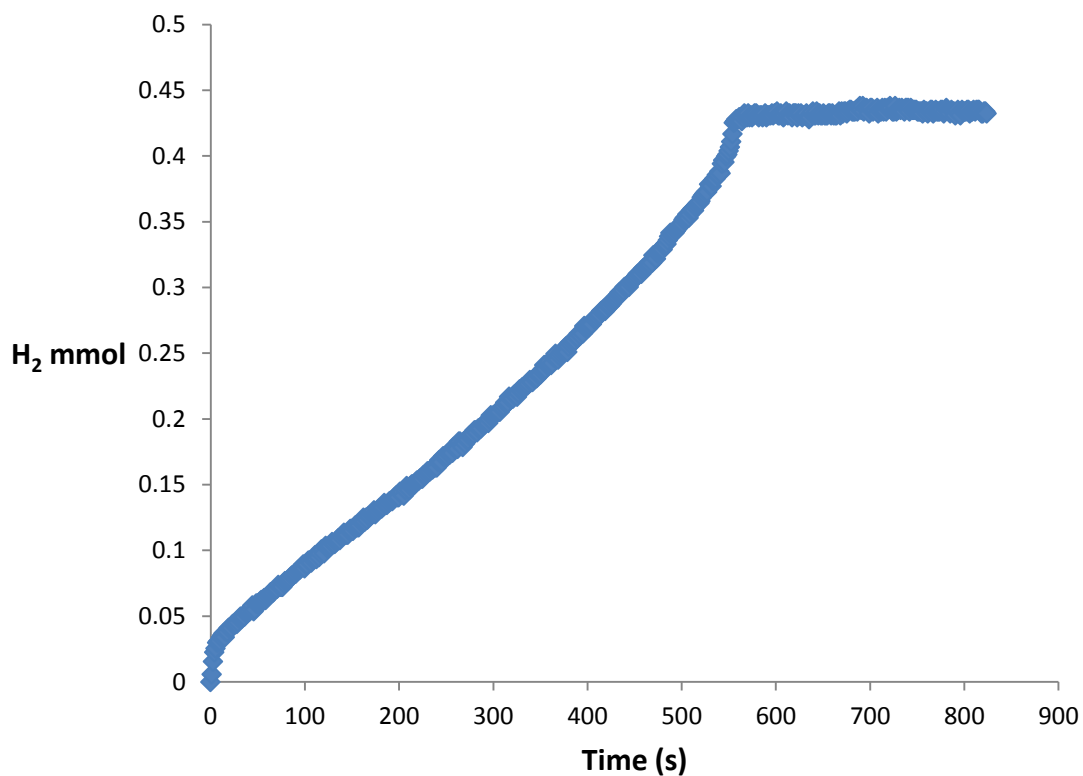


Figure S61. Monitoring the amount of H₂ released in the catalytic dehydrocoupling of NMe₂H·BH₃ and N^tBuH₂ with 0.5 % of complex **1**.

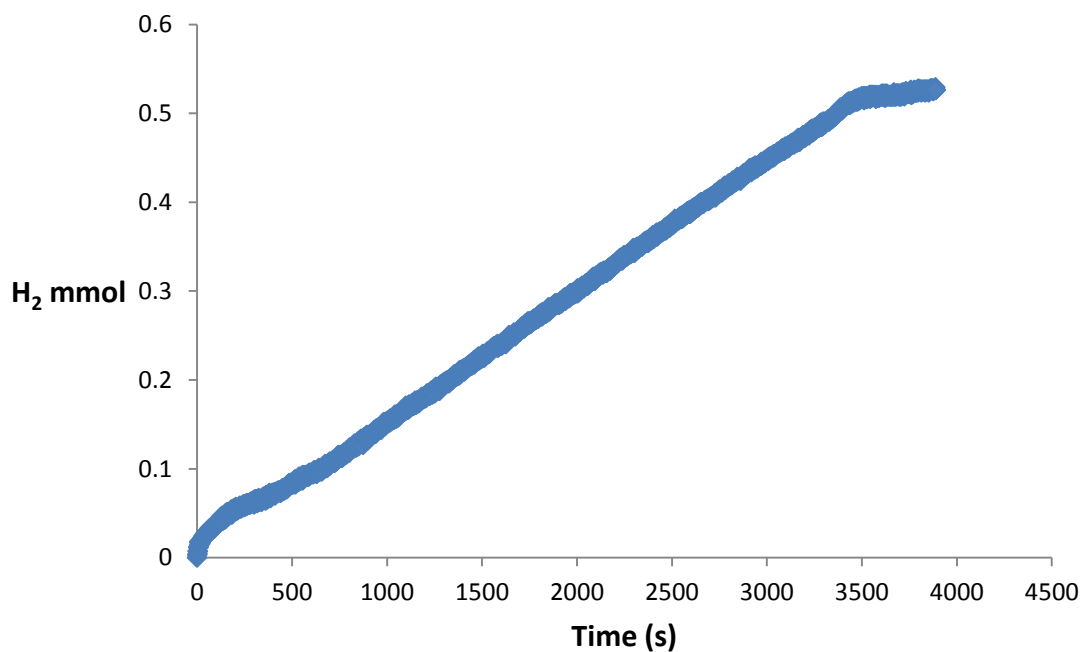


Figure S62. Monitoring the amount of H₂ released in the catalytic dehydrocoupling of N^tBuH₂·BH₃ and N(CH₂)₄H with 0.5 % of complex **1**.

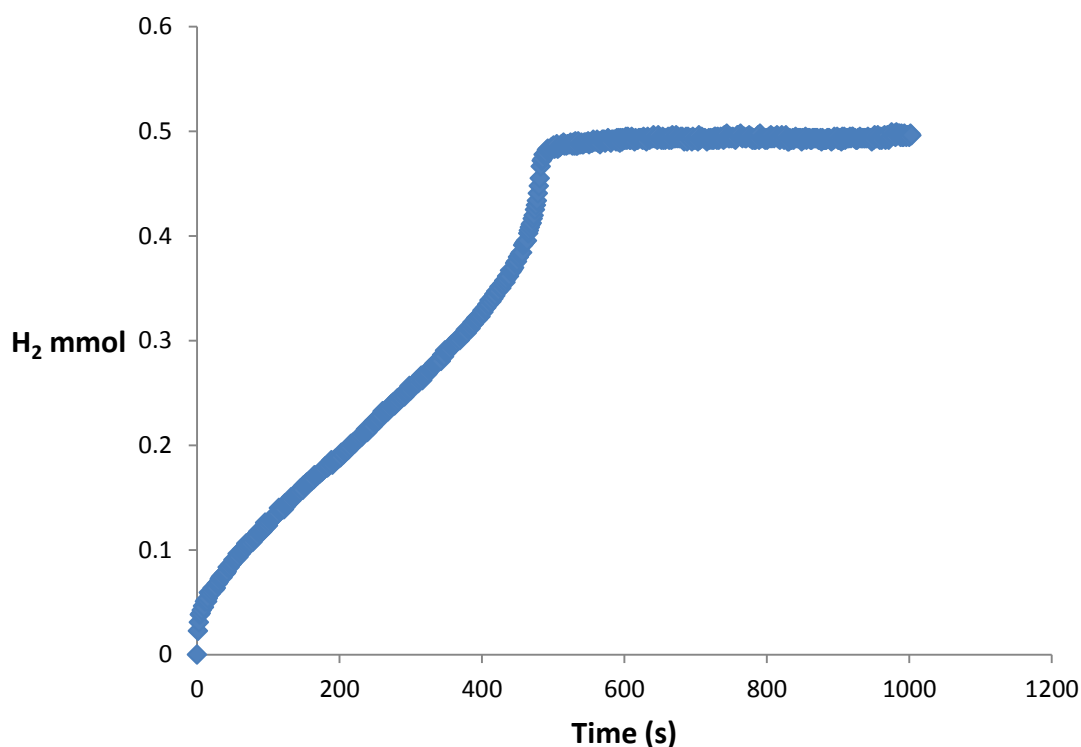


Figure S63. Monitoring the amount of H₂ released in the catalytic dehydrocoupling of NMe₂H·BH₃ and NEt₂H with 0.5 % of complex **1**.

7. X-ray crystal structure determination of complex **3c**.

Crystals appropriate for X-ray analysis were obtained using liquid diffusion techniques. The details X-ray single-crystal diffraction experiments are given in Table S1 in the Supporting Information, and molecular structure is shown in Figures 1.

Crystallographic data were collected at 273 K using a Bruker- Kappa Apex II Duo fully automatic single crystal x-ray diffractometer and monochromatic radiation (Cu-K α) ($\lambda = 1.54178 \text{ \AA}$). The software APEX21⁶ was used for collecting frames of data, indexing reflections, and the determination of lattice parameters, SAINT⁶ for integration of intensity of reflections, and SADABS⁷ for scaling and empirical absorption correction.

The software package WINGX⁸ was used for space group determination, structure solution and refinement. The structure was solved by direct methods using SIR2004.⁹ Solvent molecules in the crystal in the structure were highly disordered and were impossible to refine using conventional discrete-atom models. To resolve these issues, the contribution of solvent electron density was removed by the SQUEEZE/PLATON.¹⁰

Isotropic least-squares refinement on F^2 using SHELXL2013¹¹ was performed. During the final stages of the refinements, all the positional parameters and the anisotropic temperature factors of all the non-H atoms were refined. The H atoms were geometrically placed riding on their parent atoms with isotropic displacement parameters set to 1.2 times the U_{eq} of the atoms to which they are attached (1.5 for methyl groups) (except for BH_3 , which the H atoms were found from different Fourier maps and included in a refinement with isotropic parameters).

The function minimized was $[\sum w(F_o^2 - F_c^2)/\sum w(F_o^2)]^{1/2}$ where $w = 1/[\sigma^2(F_o^2) + (0.0411P)^2 + 135.6565P]$ with $\sigma(F_o^2)$ from counting statistics and $P = (\text{Max}(F_o^2, 0) + 2F_c^2)/3$.

Atomic scattering factors were taken from the International Tables for X-Ray Crystallography International.¹² The crystallographic plots were made with PLATON.¹⁰

Table S1. Crystal data and structure refinement for 3c.

Identification code	shelx	
Empirical formula	C ₅₉ H ₅₉ B ₂ F ₂₄ N ₅ Pt	
Formula weight	1510.82	
Temperature	273(2) K	
Wavelength	1.5418 Å	
Crystal system	Monoclinic	
Space group	C 2/c	
Unit cell dimensions	$a = 39.650(5)$ Å	$\alpha = 90.000^\circ$.
	$b = 13.440(5)$ Å	$\beta = 111.476(5)^\circ$.
	$c = 26.010(5)$ Å	$\gamma = 90.000^\circ$.
Volume	$12898(6)$ Å ³	
Z	8	
Density (calculated)	1.556 Mg/m ³	
Absorption coefficient	5.064 mm ⁻¹	
F(000)	6016	
Crystal size	0.27 x 0.23 x 0.17 mm ³	
Theta range for data collection	2.395 to 59.061°.	
Index ranges	-36<=h<=44, -14<=k<=14, -26<=l<=28	
Reflections collected	17182	
Independent reflections	8952 [R(int) = 0.0210]	
Completeness to theta = 67.000°	77.9 %	

Refinement method	Full-matrix least-squares on F ²
Data / restraints / parameters	8952 / 5 / 832
Goodness-of-fit on F ²	1.041
Final R indices [I>2sigma(I)]	R1 = 0.0395, wR2 = 0.0977
R indices (all data)	R1 = 0.0400, wR2 = 0.0981
Largest diff. peak and hole	1.653 and -1.030 e.Å ⁻³

7. References

1. S. Chitsaz, T. Breyhan, J. Pauls, B. Neumüller, *Z. Anorg. Allg. Chem.* 2002, **628**, 956.
2. Rivada-Wheelaghan, O.; Donnadieu, B.; Maya, C.; Conejero, S. *Chem. Eur. J.* 2010, **16**, 10323–10326.
3. Rivada-Wheelaghan, O.; Roselló-Merino, M.; Ortuño, M. A.; Vidossich, P.; Gutiérrez-Puebla, E.; Lledós, A.; Conejero, S. *Inorg. Chem.* 2014, **53**, 4527–4268.
4. M. Roselló-Merino, J. López-Serrano, S. Conejero, *J. Am. Chem. Soc.*, 2013, **135**, 10910.
5. www.manonthemoontech.com
6. BRUKER. *APEX2 and SAINT*. Bruker AXS Inc., Madison, Wisconsin, USA, (2012).
7. Sheldrick, G. M., SADABS v. 2008/1. A Computer Program for Absorption Corrections. University of Göttingen, Germany, (2008).
8. Farrugia L. J., *J. Appl. Crystallogr.* 2012, **45**, 849-854.
9. M. C. Burla, R. Caliendo, M. Camalli, B. Carrozzini, G. L. Cascarano, L. De Caro, C. Giacovazzo, G. Polidori, and R. Spagna, *SIR2004*, *J. Appl. Cryst.*, 2005, **38**, 381.
10. Spek A. L. *PLATON: A Multipurpose Crystallographic Tool*; University of Utrecht, The Netherlands, (2008).
11. Sheldrick G. M., *SHELXL2013: Program for the Refinement of Crystal Structures*; University of Göttingen: Göttingen, Germany, (2014).
12. *Tables for X-Ray Crystallography*; Kynoch Press, Birmingham, U.K., Vol. IV (present distributor: Kluwer Academic Publishers; Dordrecht, The Netherlands, (1974).